

**POWER DEMAND AND SUPPLY ALLOCATION USING INHERENT
STRUCTURAL THEORY OF NETWORK SYSTEMS AND VOLTAGE
STABILITY INDEX BASED ON MULTI-BUS REACTIVE POWER LOADING**



By
Mutuku Peter Munyao
218088282

A dissertation submitted in fulfillment of the requirements for the degree of
Master of Science in Electrical Engineering
College of Agriculture, Engineering and Science, University of KwaZulu-Natal

2021

Supervisor: Prof. John T. Agee

Co-supervisor: Dr. Remy Tiako

DECLARATION 1 - PLAGIARISM

I, Mutuku Peter Munyao, declare that;

1. The research reported in this thesis, except where otherwise indicated, is my original research.
2. This thesis has not been submitted for any degree or examination at any other university.
3. This thesis does not contain other persons' data, pictures, graphs or information unless expressly acknowledged as being sourced from others.
4. This thesis does not contain other persons' writing unless expressly acknowledged as being sourced from other researchers. Where other written sources have been quoted, then:
 - a. Their words have been re-written but the general information attributed to them has been referenced.
 - b. Where their exact words have been used, then their writing has been placed in italics and inside quotation marks and referenced.
5. This thesis does not contain text, graphics or tables copied and pasted from the Internet unless expressly acknowledged, and the source being detailed in the thesis and the References sections.

Signed

Date

.....

21th /AUGUST/2021

.....

As the candidate's Supervisor, I agree to the submission of this dissertation.

Signed

Date

.....

25/03/2022

.....

DECLARATION 2 - PUBLICATIONS

The following papers were published in the 2021 IEEE PES/IAS PowerAfrica conference proceedings:

Publication 1

P.M. Munyao, J.T. Agee and R. Tiako, “Generator Reserve and Load Capacity Allocation Using Ideal Generator Contribution Index.” *8th Annual IEEE PowerAfrica Conference*, Nairobi, Kenya, August 2021.

Publication 2

P.M. Munyao, J.T. Agee and R. Tiako, “Voltage Stability Index Based on Multi-bus Reactive Power Loading.” *8th Annual IEEE PowerAfrica Conference*, Nairobi, Kenya, August 2021.

Signed

Date

.....

25/03/2022

.....

ACKNOWLEDGEMENTS

First and foremost, I am grateful to God for His love and unconditional grace, which has guided my passion and sustained me through this momentous phase of my existence.

I would immensely thank my supervisor, Professor John T. Agee, for believing that all that I needed was at my disposal and for giving guidance in my research activities. In addition, great appreciation goes to my co-supervisor, Dr. Remy Tiako, for the support and academic opportunities granted as part of training.

I am grateful for the Research Grant by South Africa's National Research Foundation, Grant No: 123444.

Special thanks to Dr. Peter Akuon for your support and belief in my research pursuits. I also acknowledge my father and family at large for the financial backing amidst the prevalent pandemic conditions.

Much appreciation to Eng. Kamau Njuguna for graduate mentorship and training that aided in gaining much insight into what the engineering industry entails.

I sincerely thank all my allies and acquaintances for the moral support offered and the University of Kwa-Zulu Natal for facilitating my research.

ABSTRACT

Power availability is a crucial factor in determining new load centers. There is a need for adequate power reserve and maximum load capacity allocation to ensure continued power demand and supply electrical systems. In modern interconnected power systems, a high peak load power demand is met by the contribution of the available generator units. There is an urgency to solve the challenges arising from interconnected network configurations such as the loss of generation, inadequate supply capacity to meet load demand during peak time, transmission losses and significant voltage drop at the heavily loaded buses. This dissertation investigates the influence of inter-connected load buses on the system's voltage profile and the electrical proximity from generation sites to load centers as captured by the *Y-admittance* matrix. The inherent structural theory of networks was used in determining the required power reserve and load capacity allocation using the ideal generator contribution index. PowerWorld simulator, Dig SILENT Power Factory and MATLAB were used as simulation and presentation tools for the modified IEEE 14 bus system and the Southern Indian 10 bus system. From the analysis of the results, much of the load capacity needed for electrical load growth is feasible for the bus that is most electrically proximal to a high-rated power source. The use of the ideal generator contribution index exploits the structural properties of the network. That being the case, its advantages include minimum expansion of existing structures and minimal transmission active power losses. Also, in this dissertation, a *V-Q* curve characteristic approach was used to identify the weak load buses in an interconnected power system. This was done by simulating uniformly distributed multi-bus loading conditions and the conventional analysis of the sole bus loading method in a power network system up to the minimum acceptable per unit voltage point. This led to the formulation of a novel *V-Q* curve-based index. The voltage critical multi-bus index is a variable state-based index. This index was compared with the self-sensitivity index of the reduced Jacobian matrix and the 'load structural electrical attraction region' index of the inherent structural theory of power networks, giving a deeper insight into the system characteristics under light and heavy loading states.

Table of Contents

DECLARATION 1 - PLAGIARISM	ii
DECLARATION 2 - PUBLICATIONS	iii
ACKNOWLEDGEMENTS	iv
ABSTRACT.....	v
LIST OF FIGURES	viii
LIST OF TABLES	ix
NOMENCLATURE	x
CHAPTER 1 - INTRODUCTION.....	1
1.1 Introduction.....	1
1.2. Research Objectives.....	2
1.3. Key Research Assumptions	2
1.4. Contributions of the Study	2
1.5. Organisation of the Dissertation	2
CHAPTER 2 – LITERATURE REVIEW	3
2.1. Introduction.....	3
2.2. Reserve Capacity Allocation.....	3
2.3. The Ideal Generator Contribution Index	5
2.4. System Voltage Indices.....	6
2.5. Voltage Critical Bus Index (<i>VCBI</i>)	7
2.6. V-Q Curves	8
2.7. Conclusion	8
CHAPTER 3 – METHODOLOGY	9
3.1. Introduction.....	9
3.2. Ideal Generator Contribution Index	9

3.3. Generator Reserve and Load Capacity Allocation by Use of Ideal Generator Contribution Index .	11
3.4. Deriving $\Delta V/\Delta Q$ Self-sensitivities from Reduced Jacobian Matrix.....	14
3.5. Derivation of Multi-Bus V-Q curve Based Index	15
3.6. Conclusion	16
CHAPTER 4 – SIMULATIONS AND RESULTS	17
4.1. Introduction.....	17
4.2. Test System Models.....	17
4.3. Simulation and Results for Generator Reserve and Load Capacity Allocation Using Ideal Generator Contribution	19
4.3.1. Case Study 1: 10 Bus Southern Indian Network.....	19
4.3.2. Case Study 2: The Modified IEEE 14 Bus System.....	24
4.4. Simulation and Results for Voltage Stability Index Based on Multi-bus Reactive Power Loading	29
4.4.1. Case Study 1: 10 Bus Southern Indian Network.....	29
4.4.2. Case Study 2: IEEE 14 Bus System.....	32
CHAPTER 5 – CONCLUSION AND RECOMMENDATIONS	35
5.1. Conclusion	35
5.2. Recommendation for Future Work	35
REFERENCES	36
APPENDIX A.....	40
APPENDIX B	47
APPENDIX C	49
APPENDIX D.....	51

LIST OF FIGURES

Figure 3.1: V-Q curve of a sole bus loading-----	15
Figure 3.2: V-Q curve of a particular bus for sole bus loading and multi-bus loading-----	15
Figure 4.1: Equivalent Southern Indian Network System [18].....	17
Figure 4.2: Single-line diagram of the modified IEEE 14 Bus System.....	18
Figure 4.3: Single-line diagram of the IEEE 14 Bus System.....	18
Figure 4.4: Graphical representation of generator power contribution to meet sole bus load demand in Southern Indian Network using MATLAB software.....	19
Figure 4.5: Graphical representation of generator power contribution to meet uniformly distributed multi-bus load demand in Southern Indian Network using MATLAB software	19
Figure 4.6: Generator power contribution to meet sole bus load demand in the modified IEEE 14 Bus System.....	24
Figure 4.7: Generator power contribution to meet uniformly distributed multi-bus load demand in the modified IEEE 14 Bus System.....	24
Figure 4.8: Results showing generator contribution to meet network’s reactive power demand in IEEE 14 Bus System using Dig-SILENT Power Factory.	25
Figure 4.9: Results showing base case load-supply in the modified IEEE 14 Bus System using Dig-SILENT Power Factory.....	25
Figure 4.10: Results showing load-supply when bus 8 is at 20 MW, in the modified IEEE 14 Bus System, using Dig-SILENT Power Factory.....	26
Figure 4.11: Results showing power supply for all units when Generator 4 is set the maximum at 52 (MW), in the modified IEEE Bus System using Dig-SILENT Power Factory	26
Figure 4.12: V-Q curves comparison for all load buses when only bus 5 is loaded at Southern Indian Network System.....	29
Figure 4.13: V-Q curves comparison for all load buses when only bus 6 is loaded at Southern Indian Network System	29
Figure 4.14: V-Q curves comparison for Southern Indian Network System when all buses are loaded at a time.....	30
Figure 4.15: V-Q curves comparison for Southern Indian Network System when all buses are loaded simultaneously and uniformly	30
Figure 4.16: V-Q curves comparison for IEEE 14 bus system when each bus is loaded individually at a time.....	32
Figure 4.17: V-Q curves comparison for IEEE 14 bus system when all buses are loaded simultaneously and uniformly.....	33

LIST OF TABLES

Table 3.1: Ideal Generator Contribution matrix, $ F_{LG} $	11
Table 4.1: Ideal Generator Contribution for Southern Indian Network, $ F_{LG} $	20
Table 4.2: Load Demand and Generation Schedule for Base Load Case, Southern Indian Network [22].....	20
Table 4.3: Simulation Results Showing Base Case Load-Supply in Southern Indian Network using Power World Simulator	21
Table 4.4: Load Demand and Generation Schedule When Bus 7 Load Demand Is Projected To 350 MW, In Southern Indian Network.....	21
Table 4.5: Ideal Generator Contribution for IEEE 14 Bus System, $ F_{LG} $	22
Table 4.6: Simulation Results Showing Load-Supply For Bus 7 At 350 (MW) In Southern Indian Network Using Power World Simulator	22
Table 4.7: Permissible Load Demand at Bus 5 and Generation Schedule When Generator 2 Maximum Supply Is 120 MW, In Southern Indian Network.....	23
Table 4.8: Simulation Results Showing Permissible Load Capacity at Bus 5, When Supply from Generator 2 is Set Maximum at 120 (MW), in Southern Indian Network Using Power World Simulator.....	23
Table 4.9: Load Data and Generation Schedule for Base Load Case, in the modified IEEE 14 Bus System Using Ideal Generator Contribution Index.....	26
Table 4.10: Load Data and Generation Schedule when Bus 8 Load Demand is Projected to 20 MW in the modified IEEE 14 Bus System.....	27
Table 4.11: Permissible Load Demand at Bus 12 and Generation Schedule when Generator 4 Maximum Supply is 52 MW In the modified IEEE 14 Bus System.....	28
Table 4.12: Load Structural Electrical Attraction Region for the Southern Indian Network [20].....	31
Table 4.13: Eigenvalues of $\Delta V/\Delta Q$ Self-Sensitivities Using the Reduced Jacobian Matrix for Southern Indian Network System.....	31
Table 4.14: VCMBI for the Southern Indian Network System	32
Table 4.15 Load Structural Electrical Attraction Region for IEEE 14 Bus System	33
Table 4.16: Eigenvalues of $\Delta V/\Delta Q$ Self-Sensitivities Using the Reduced Jacobian Matrix for IEEE 14 Bus Network System.....	34
Table 4.17: VCMBI for the IEEE 14 Bus Network System.....	34

NOMENCLATURE

RED	Relative electrical distance
MW	Megawatts
MVAR	Mega volt ampere reactive
$V-Q$	Voltage versus Reactive Power
ORDC	Operating reserve demand curve
IRM	Installed reserve margin
PSI	Power stability index
VSI	Voltage stability index
V_{cr}	Critical voltage
ISTN	Inherent structural theory of networks
ΔV	Voltage deviation
ΔQ	Reactive power deviation
VCMBI	Voltage critical multi-bus index

CHAPTER 1 - INTRODUCTION

1.1 Introduction

Electricity demand and supply must be closely matched in electrical power systems to avoid adverse consequences leading to grid shutdown [1]. The reserve capacity is utilized to meet demand if a particular generator is isolated from the grid or if there is supply disruption [1] [2]. Adequate allocation of electrical power reserves ensures that all forecasted load consumption is duly met [3] [4]. An operating reserve offers a safety margin that helps in ensuring the reliability of the power system network despite variability in the electric load and the renewable power supply. The term spinning reserve is more commonly used to mean *operating reserve*. This is so because fuel cells, batteries and the grid can offer this type of reserve although they do not spin [5] [6]. In some regions, wind is a dispatchable resource and operators can purposely control output to ramp the plant up or down (to match load or provide reserves) [7] [8]. In power system networks, forecasting of electrical loads growth, which may be projected to a period of up to several decades, is a crucial step in the planning and developing generation, transmission and distribution systems. Power system engineers use the results of such forecasts to efficiently coordinate resources to meet power demand while providing an acceptable level of power quality and reliability [9].

Besides the power supply and load demand matching challenge in grid systems, the lack of sufficient reactive power in an electrical power system, together with the continuous upsurge in electrical load demand, are the key factors among many others, contributing to the occurrence of voltage collapse in modern power systems [10] [11]. The emerging industrial load centers (which heavily absorb reactive power) and massive assimilation of the intermittent distributed generator sources have led to a broader and uncertain range of grid operating conditions. The resultant consequence is reduced voltage stability margins when optimum coordination is not done [12]. This being so, the proper planning, continuous monitoring and the control of power systems through voltage stability indices is urgently needed [13].

Voltage stability analysis entails assessing the electrical network's weak, unstable or uncontrollable areas that may pose a risk to the future of load growth due to unexpected voltage collapse [13] [14]. Voltage stability indices function to situate the current operation of a power system, predict future changes to the nature of the system, and evaluate a long-run development trend within pre-defined circumstances [13]. Voltage stability may be enhanced during the design and power system operation phases [13] [14]. Two main categories of voltage stability indices include; singular value-based and variable (parameter) based indices [13]. The extensive calculation time and limitations for radial systems are the main disadvantages of the singular value-based indices. On the other hand, the variable-based indices are helpful during the analysis at instances of heavy load conditions [13] [14].

1.2. Research Objectives

In the existing literature, standards and analytical methods for determining the operating reserve requirements for various systems have been undertaken. The requirements include the capacity amounts, speed at which they should respond, how they should react, when and how soon they should be ready for subsequent usage [3] [4]. In this dissertation, the proposed approach for the reserve allocation, allowable future load calculating and load supply matching differs from the existing methods by using the network's structure as captured by the *Y-admittance* matrix [15]. The method uses the ideal generator contribution index derived from the inherent structural theory of networks. The distinctive property of the ideal generator contribution matrix is that its row summation is bound to a value approximate to unity and apportions load demand according to their relative electrical proximity from generators in the power system network. The network structure, characterized by the interconnection through transmission lines, inherently influences losses and the voltage profile. This approach utilizes the relative electrical distance to necessitate planning with a minimum expansion of the existing network structure and minimal power loss to identify buses for additional generation units.

Additionally, this dissertation aims to use a V-Q curves approach method within pre-defined voltage limits (in per unit) along the stable voltage region to develop an index to predict the stiffness of a bus to voltage drop. The V-Q curves characteristics plotted while considering uniformly distributed loading (across all buses) and sole bus loading to determine (by use of a new index) how fragile and vulnerable a bus is to voltage drop as a result of being a supply node to a considerably heavy reactive electrical power load (up to any stipulated minimum per unit voltage before total voltage collapse). This study aims to contribute to the overall planning and operation of a stable electrical power system by using the ideal generator contribution index and the novel voltage critical multi-bus index.

1.3. Key Research Assumptions

The following assumptions were made;

- The generator units used in the investigation represent the base load supply units.
- Most of the load power demand is inductive reactive (MVARs) for heavy industrial machines and the growing usage of home appliances.
- A generator bus may include several units, where some specific supply units are active/online and the offline units meet the requirements needed for future power generation scheduling.
- No reactive power compensators are installed in shunt/parallel unless modelled to cater to the source and sink nature of the power system elements.

1.4. Contributions of the Study

The contributions of the study are as follows:

- The concept of relative electrical distance, based on the network's structure (to harness the benefits of minimal expansion requirements and fewer transmission losses), has been used to allocate power reserves and electrical loads. The minimum reserve capacity is slated according to the calculated values of the derived formula based on the ideal generator contribution index. In our study (in the case of the Southern Indian Network), when the load at bus 7 is projected from 250 MW to 350 MW, generator 1 increases its supply by 39 MW, generator 2 by 11.75 MW and generator 3 by 43.4 MW. The permissible load demand at bus 5, when generator 2 is restricted to a maximum power supply of 120 MW, gives a value of 240.5 MW from 150 MW. That being so, generator 1 is scheduled to supply 57.35 MW as additional power while generator 3 is set to supply 27.94 MW as extra power (reserve power).
- The simulated and calculated results of the power demand for single/sole bus load demand and the uniformly distributed load across all buses have been presented in this study. Results analysis show deviations of the order 0.01 in magnitude (for the ideal generator contribution index), further cementing the viability of the inherent structural theory of networks indices.
- A new index based on $V-Q$ curves plot characteristics has been derived. This necessitates the investigation of network systems under heavy reactive power loading conditions. The voltage critical multi-bus index and the inherent structural theory of networks (the load structural, electrical attraction region) index identified bus 6 as the weakest bus.

1.5. Organisation of the Dissertation

The remaining sections of the dissertation are as follows:

Chapter 2 gives the literature review of the existing research works on reserve power allocation, the inherent structural theory of networks, and voltage stability indices. Chapter 3 contains the methodology used for developing the ideal generator contribution index from the inherent structural theory of networks and the new formulations for power reserve and load capacity allocation. Additionally, the application of $V-Q$ curves plot characteristics in deriving the novel index, the voltage critical multi-bus index, is demonstrated. Chapter 4 analytically presents, compares and discusses the simulated and calculated results. Chapter 5 is the conclusion and future work recommendation; this chapter summarises the objectives of the research work.

CHAPTER 2 – LITERATURE REVIEW

2.1. Introduction

There is a great need to ensure that power generation matches load demand in the existing power systems while also providing an adequate reserve that would guarantee overall stability during its operation [9]. Over the recent years worldwide, continued growth in electricity demand (having not been matched with an equivalent growth in generation) has eroded the reserve margins, leading to a scenario where the power system is operated at its limits [16]. Under these circumstances, a sudden loss in load often leads to increased rotor speeds, resulting in unwanted mechanical oscillations in the generator and transient variations in frequency and voltage, especially in a less inter-connected network system [17]. On the other hand, a loss of large generating units at instances of fewer reserve margins can lead to a frequency droop due to network overloading [16] [17]. Therefore, there is an urgent need to plan, calculate, add enough reserve capacity to avoid a supply shortage if one of the primary power plants cannot operate as usual or an emergency increase in demand occurs [2] [3]. Since a voltage collapse at a bus can lead to significant deviations in rotor angle and output frequency, the same way a significant frequency change may lead to large changes in voltage magnitude, accurate ways of identifying weak nodes/buses in an interconnected system are required.

2.2. Reserve Capacity Allocation

The *Required operating reserve* is the least amount of operating reserve that the power system must be capable of providing. In the modern power systems, the inter-connectedness of its network structure provides the needed reserve capacity for the system thus increasing the supply reliability. Inadequate reserve capacity might lead to frequent unplanned load shedding e.g. in South Africa [18]. A search for ways to produce extra power without building new power stations led to the refurbishment of its older units, contributing to the needed power generation during peak and high load demand even though they were small in size [18].

According to the author [19], the allocation methods of the reserve can be classified into three of the following: the sequence allocating method, the allocation based on the frequency of blackout occurrence and the allocation based on the maximum output of large generators that are online each hour. For the sequence allocation method, the critical feature is that the unit's reserved share is related to its rated capacity. The larger the unit's rated capacity is, the more it shares the reserve, and vice versa [19]. On the allocation based on the frequency of blackout occurrence, the method is simple; however, it requires the acquaintance of blackout statistics. The analysis of the cause of a blackout must be performed to judge if it

is a contingency. The method also has some disadvantages, including difficulty in ascertaining a large unit's fault since such occurrences are incidental. Also, the power reserve demands are usually determined beforehand for most power systems. In the third method, which is based on the maximum output of large generators online hourly, the maximum capacity of each online unit in the given period is recorded. This method is helpful for application and understanding since the online measure of the units' power outputs is simple. The unit's actual running capacity, not the rated capacity, is used in computation [19].

According to the author [5], calculating the required operating reserve for each time step based on the values and constraints formula is demonstrated. Since operating reserve caters to system's increase in the load or decrease in the renewable power output (varying generation output), the required operating reserve can be modelled as a function of both the load demand and the varying power. According to authors in [4], the rules guiding the allocation of operating reserves employed for the active power balance have been established through years of experience in various global regions of grid operation. It has also been noted that power systems differ in the following aspects: the size and frequency response characteristics, load characteristics and the transmission network. The approach to dealing with risk can also be quite different for a particular system operator [4].

Authors in [20] developed a dynamic simulation framework to assess the performance of ORDC (Operating reserve demand curve) in safeguarding resource adequacy and system reliability in energy-only electricity markets. Two significant indices are considered: IRM. (Installed reserve margin) and the generator's profit indices. Randomly-generated load data has been used to simulate the demand uncertainty.

From these previous reserve allocation and management methods, there is a need to fill the gaps of failing to anticipate reserve demand in advance, transmission losses, and planning based on load characteristics. In this work, the ISTN's (Inherent Structural Theory of Networks) index, Ideal Generator Contribution index, has been chosen as an alternative to previous methods, excluding in-depth analysis of the economic aspect of contingencies and power system operations. This index can be applied to locate potential buses for adding new reserves by calculating the amount of power reserve needed and identifying the units with high power penetration to the system. Implementing the ideal generator contribution is advantageous because it is faster than conventional power flow methods [15]. In addition, it provides a way to relate the system behavior (relative electrical distance and power contribution to meet load demand) to how power lines and buses influence each other [21].

2.3. The Ideal Generator Contribution Index

The concept of path matrix [13] or relative electrical distance has been used to formulate the T-index by authors in [22]. On further developments of this idea, another index was developed using the theory of the inherent power system characteristics [15] [23] and is known as the ideal generator contribution index [15]. This index is hinged on the inter-connection of buses as captured in the network's Y -admittance matrix [15]. By use of ohms law $I = Y*V$, the interconnected network was modelled using its Y -admittance.

$$Y_{\text{Partitioned admittance matrix}} = \begin{pmatrix} Y_{GG} & Y_{GL} \\ Y_{LG} & Y_{LL} \end{pmatrix} \quad (2.1)$$

Equation (2.1) is partitioned in line with source (generator) and sink (load). Authors in [15] obtained a simple equation of sub-matrices presented as follows

$$F_{LG} = - Y_{LL}^{-1} Y_{LG} \quad (2.2)$$

The absolute value of the matrix F_{LG} denotes the ideal generator contribution [15] [22]. This matrix captures the ratio that a particular generator supplies power to meet load demand with respect to the online pool of generators in a power system network. It is a linearized approach that employs circuit laws to solve a power flow problem. Traditionally, the solutions to load flow are solved by iterative techniques and have not offered information regarding the system structure as per authors in [15]. This behoves power system engineers to apply physical principles to understand better how variables interplay in a network structure in harmony with fundamental circuit laws. With that in mind, this has culminated in developing the ideal generator contribution index by authors in [15] [22].

According to authors in [24], when locating new generator buses for a maximum contribution of power into the system, this index effectively ensures that line overloading does not occur, thus necessitating planning within existing transmission corridors with the negligible expansion, leading to overall system stability [22] [25]. Furthermore, this approach results in less active power losses when implemented [22]. However, factors like voltage drop and the effect of large reactive loads haven't been captured in this index; thus, there was a need to go ahead and develop an index based on the non-linearity property of most system loads. This leads to a study on system voltage indices, in a quest to improve the general power system's stability, by identifying weak buses (for reactive power compensation), leading to the relief of power generation and reserve units. The resultant complete work (in this dissertation) is vital in ensuring a

complementary approach (in analysis and design) to solving system stability problems [13] by using inherent structural and variable-based models.

2.4. System Voltage Indices

According to authors in [26, 27, 28], the purpose of voltage stability indices is to locate the current operating voltage of a power system, forecast future deviations and approximate a long-run trend within pre-defined conditions [29, 30]. An in-depth analysis of voltage stability indices has been done in the previous three decades [13, 31, 32]. These authors classify indices into two major types: singular value-based and variable-based indices. The singular value-based (power flow Jacobian) indices can be used to predict a system's critical operating point. They can be reckoned as a proper tool for estimating instability and power transfer capability under static analysis conditions [13]. The lengthy calculation and limited use on radial systems are the main disadvantages of these indices.

The Sensitivity analysis indices (variable-based) utilize active and reactive power deviations to approximate the safety margin between a system's operating and collapse point. In terms of the prediction accuracy in offline applications and high sensitivity near the critical operating point, this index is deemed less accurate when compared to other categories of indices. However, it is worth noting that this index is an excellent tool in estimating a power system's steady-state condition using visual graphical representations of P–V and P–Q curves [33].

According to [13], it has been proven that there are certain indices, which are profoundly identical, but different from the driven point of view [14]. In other words, their results are complementary each in mutual concord. Also, an index which has a lower ranking when it comes to compliance with other indices does not suggest that the index is ineffectual since each index is best functional for a specific application. In the literature [30, 32], when the same system under investigation is subjected to a heavy load in a strained situation [34], the $\Delta V_i/\Delta Q_i$ and $\Delta V_i/\Delta P_i$ sensitivity indicators play an important role in the system's voltage collapse prediction [35] [36].

2.5. Voltage Critical Bus Index (VCBI)

A recent model of system parameters (V and Q) has been developed in [11]. When V_n is taken to represent the load bus nominal voltage and V_b is the voltage of load bus b established during the power flow solution [11]. Then the change in the reactive power variation at each load bus of the system is ΔQ , with M_T being the total number of step size or iterations taken by each load bus to reach the maximum load-ability.

Authors in [11] have determined that the load bus that has maximum *VCBI* with the lowest reactive power load-ability or lowest value of M_T is the most critical bus.

$$(VCBI_b)_{k=1\dots M_T} = \max_{b=1\dots NL} \frac{\left| (\sum_{b=1}^N (\Delta b))_{k=1\dots M_T} \right|}{(M_T)_b * (Q_{max})_b} \quad (2.3)$$

Where

$$(Q_{max})_b = \sum_{b=1}^N (\Delta Q_b)_{k=1\dots M_T} \quad (2.4)$$

And

$$\left| (\Delta_b)_{k=1\dots M_T} \right| = \left| \frac{(V_n - V_b)_{k=1\dots M_T}}{V_n} \right| \quad (2.5)$$

Authors in [11] used sensitivity analysis indices which are parameters (variables) based to form the *voltage critical bus index (VCBI)*. This concept has implemented the conventional approach to determine the point of voltage instability. Since voltage stability in power systems is hugely dependent on the reactive power availability at system's load buses, the conventional way of identifying critical buses is normally done by subjecting the system to gradual reactive power load variation at each load bus until the point of collapse. This is typically realised by taking one bus at a time until the maximum acceptable load on a specific load bus is reached [11]. However, it can be inferred that this approach is limited in its use when the power system network is loaded across multiple buses at the same instance since all load buses influence each other in an inter-connected system. This leads to the derivation of an alternative index in this research work by using V-Q curves (similar in the principle of formulation) to cater to the effect of adjacent buses on the voltage drop of a particular bus.

2.6. V-Q Curves

Authors in [37] ascertained that the V-Q method was advanced owing to difficulties in power flow program convergence of stressed cases. Advantages include: First, convergence is generally not a major issue, even on the “unstable” left side of the curve. Secondly, the method is fast and for a slight variation in the scheduled voltage, convergence takes only a few iterations with the conditions from the preceding case taken as the starting point. Thirdly, the reactive power shunt compensation requirements are approximately given and reactive power compensation characteristics (capacitor bank or SVC) can be superimposed on the V-Q system characteristic. Fourthly but not least, the slope of the curve indicates voltage “stiffness,” [37] a property that can be used to predict a bus susceptible to voltage collapse.

2.7. Conclusion

The approaches to reserve allocation purposely to meet demand have been discussed. The link between supply reserve, emergency load demand and power supply matching and voltage stability has also been identified for research to enhance overall power system stability and minimize transmission losses. This dissertation aims to mathematically convey, based on ideal generator contribution, the required generator reserve and load capacity with respect to generator rated output. The scope of this dissertation does not examine the economics of generation and the cost of adding new units to the system. The modelling challenge posed by buses with both source and sink configurations can be eliminated by reducing the network under investigation into its equivalent source and sink networks, then working on the resultant networks. The distinctive advantages of using the ideal generator contribution index include; less computation time, effectiveness in ensuring that the line overloading does not occur, minimum infrastructure expansion and its implementation translate to having less active power losses. This dissertation also aims to use *V-Q* curve characteristics of uniformly distributed loading and sole bus loading to determine (by use of an index) how fragile and vulnerable a bus is to voltage collapse (as a result of being a termination node to a considerably heavy reactive electrical power equipment). Adequate reactive power compensation in the susceptible regions ensures that active power reserves are not depleted while supplying such critical buses in the power system network.

CHAPTER 3 – METHODOLOGY

3.1. Introduction

This chapter centres on the methodology and mathematical formulations implemented to allocate and identify (in a strained power network system) the required generator reserves (or the additional power supply capacity). The maximum power demand permissible at a particular load bus is mathematically defined while considering the available generation capacity based on the ISTN's (the ideal generator contribution) index. In addition, the derivation of the $\Delta V / \Delta Q$ self-sensitivities (from the reduced Jacobian matrix by eigenvalue method) is done for comparison purposes with the ISTN's (load structural electrical attraction region) index. Also, a new index was derived (the voltage critical multi-bus index) based on the plot characteristics of the $V-Q$ curves, contributing to the power system stability improvement by identifying the weak buses for reactive power compensation.

3.2. Ideal Generator Contribution Index

For structurally complex circuits [38], such as the interconnected power systems networks, it is much simpler to use the Y -admittance in order to utilize the links between adjacent buses (for identifying essential structural information related to conventional power flow solutions) [15] [38]. The ideal generator contribution index is derived from the Y -admittance matrix through the source (generator bus) and sink (load bus) partitioning method [15, 23]. For a given power system, the network admittance matrix can be conveyed as follows [39]:

$$Y = \begin{pmatrix} Y_{GG} & Y_{GL} \\ Y_{LG} & Y_{LL} \end{pmatrix} \quad (3.1)$$

Using ohm's law $I = Y^*V$, the Schur complement of Y_{LL} is derived as follows:

$$\begin{pmatrix} I_G \\ I_L \end{pmatrix} = \begin{pmatrix} Y_{GG} & Y_{GL} \\ Y_{LG} & Y_{LL} \end{pmatrix} \begin{pmatrix} V_G \\ V_L \end{pmatrix} \quad (3.1a)$$

Expanding (3.1a)

$$I_G = Y_{GG}V_G + Y_{GL}V_L \quad (3.2)$$

$$I_L = Y_{LG}V_G + Y_{LL}V_L \quad (3.3)$$

Where I_G, I_L are complex bus injection currents for the generator and load respectively [15]; V_G, V_L are complex bus voltage injection vectors for the generator and load respectively [15]. The Y -admittance is a square matrix of dimensions $(G + L) \times (G + L)$ [15] [23], Y_{GG} is a square matrix of dimension $G \times G$

representing the connectivity between the generator buses [15]. Y_{GL} is a $G \times L$ matrix relating the generator to load buses, Y_{LG} is the transpose of Y_{GL} , Y_{LL} is a square matrix of dimension $L \times L$ containing the connectivity between load buses [15] [21]. G is the number of generator buses and L is the number of load buses in the network respectively [15] [39].

Pre-multiplying (3.3) by Y_{LL}^{-1} and making V_L the subject, we get;

$$V_L = Y_{LL}^{-1} I_L - Y_{LL}^{-1} Y_{LG} V_G \quad (3.4)$$

Substituting (3.4) in (3.2)

$$I_G = Y_{GL} Y_{LL}^{-1} I_L + (Y_{GG} - Y_{GL} Y_{LL}^{-1} Y_{LG}) V_G \quad (3.5)$$

Equations (3.4) and (3.5) can be expressed in matrix form [15] as;

$$\begin{pmatrix} V_L \\ I_G \end{pmatrix} = \begin{pmatrix} Z_{LL} & F_{LG} \\ K_{GL} & S_{GG} \end{pmatrix} \begin{pmatrix} I_L \\ V_G \end{pmatrix} \quad (3.6)$$

Where

$$Z_{LL} = Y_{LL}^{-1} \quad (3.7a)$$

$$F_{LG} = - Y_{LL}^{-1} Y_{LG} \quad (3.7b)$$

And

$$K_{GL} = Y_{GL} Y_{LL}^{-1} \quad (3.8a)$$

$$S_{GG} = Y_{GG} - Y_{GL} Y_{LL}^{-1} Y_{LG} \quad (3.8b)$$

Z_{LL} denotes the total load impedances and accounts for the total load losses, K_{GL} is the negative transpose of F_{LG} . S_{GG} is the Schur compliment of Y_{LL} and represents the generator structural electrical attraction region. Y_{LL} and the Y -admittance matrix and can be related as follows [15]

$$\det Y = \det Y_{LL} \det S_{GG} \quad (3.8c)$$

To identify all ISTN indices [15], algebraic manipulation of (3.1a) gives the following:

$$\begin{pmatrix} V_G \\ I_L \end{pmatrix} = \begin{pmatrix} Z_{GG} & H_{GL} \\ W_{LG} & M_{LL} \end{pmatrix} \begin{pmatrix} I_G \\ V_L \end{pmatrix} \quad (3.9)$$

Where $Z_{GG} = Y_{GG}^{-1}$ represents total generator impedances and accounts for the total generator losses [15] [15]. H_{GL} characterises the influence of generators on the load buses [15]. W_{LG} is the negative transpose of H_{GL} . $M_{LL} = Y_{LL} - Y_{LG} Y_{GG}^{-1} Y_{GL}$ is the Schur complement [15] of Y_{GG} in the partitioned Y -admittance matrix (3.1) and defines the load structural electrical attraction region [15] [15].

From (3.7b), the absolute value of the matrix F_{LG} gives the ideal generator contribution [15]. The rows and columns correspond to the load bus numbers and generator bus numbers respectively [15]. Each row element determines the ideal proportion of load bus power allocated to an equivalent generator. From the literature [15] [22], each row summation is $\cong 1$ (in the results section, the summation of the rows in $|F_{LG}|$ can ascertain this mathematical property) [15] [22]. Utilization of this property can determine load capacity and generator reserves allocation using a mathematical formulation that assigns power according to the matrix elements of $|F_{LG}|$ in a similar principle used to determine best site for generator placement by the authors in [22].

3.3. Generator Reserve and Load Capacity Allocation by Use of Ideal Generator Contribution Index

The following mathematical equations were derived and presented in this section to find the generator reserve and load capacity allocation. From the absolute value of the matrix F_{LG} , i.e. $|F_{LG}| = | - Y_{LL}^{-1} Y_{LG} |$, the elements were considered as the index values as explicated in section 3.2. The relationship between the generator buses and load buses through the Relative Electrical Distance [22] makes it possible to find the generator power output required for a particular load demand and vice versa in this dissertation.

Table 3.1: Ideal Generator Contribution matrix, $|F_{LG}|$

			Generator buses $i = 1, 2, \dots, I$					
Load buses $k = 1, 2, \dots, N$		Particular load bus number	G1 $i = 1$	G2 $i = 2$	G3 $i = 3$.	..	Total row summation (load bus k)
	k = 1	n = 4	$\chi_{ki} = \chi_{11}$	$\chi_{ki} = \chi_{12}$	$\chi_{ki} = \chi_{13}$.	..	$\chi_T \cong 1$
	k = 2	n = 5	$\chi_{ki} = \chi_{21}$	$\chi_{ki} = \chi_{22}$	$\chi_{ki} = \chi_{23}$.	..	$\chi_T \cong 1$
	k = 3	n = 6	$\chi_{ki} = \chi_{31}$	$\chi_{ki} = \chi_{32}$	$\chi_{ki} = \chi_{33}$.	..	$\chi_T \cong 1$
	k = 4	n = 7	$\chi_{ki} = \chi_{41}$	$\chi_{ki} = \chi_{42}$	$\chi_{ki} = \chi_{43}$	$\chi_T \cong 1$
	χ_{NI}	$\chi_T \cong 1$

The bus numbering starts with generator buses then load buses (this is due to the source and sink partitioning approach i.e. $n = I + 1, I + 2, \dots, N$).

To derive the generator reserve and load capacity allocation, we annotate the following as:

- χ_{ki} = A particular ideal generator contribution index value for load bus k, with k and i representing the matrix $|F_{LG}|$ row and column number respectively.
- χ_T = The row summation of all generator index values for a specific load bus k.
- g_{ki} = A particular generator's actual power contribution for a load bus k, with k and i representing the matrix $|F_{LG}|$ row and column number respectively.
- S_k = Actual load power demand at load bus k.

By letting the following

$$\alpha_{ki} = \frac{\chi_{ki}}{\chi_T} \quad (3.10)$$

It is worth noting that, $\alpha_{ki} \cong \chi_{ki}$ since $\chi_T \cong 1$. In order to calculate the actual power contribution by a specific generator to meet a designated bus k load demand, we have

$$g_{ki} = \alpha_{ki} * S_k \quad (3.11)$$

For N number of load buses, we let the total (sole generator's) power contribution to the system be G_i so that the following expression may result:

$$G_i = \alpha_{1i} * S_1 + \alpha_{2i} * S_2 + \dots \alpha_{Ni} * S_N \quad (3.12)$$

Thus

$$G_i = \sum_k^N \{ g_{ki} \} \quad (3.12a)$$

And

$$G_i = \sum_k^N \{ \alpha_{ki} * S_k \} \text{ for all } k = 1, 2, 3, \dots, N \quad (3.13)$$

For a specific load bus, let $k = n$,

$$G_i = \sum_{k \neq n}^N \{ \alpha_{ki} * S_k \} + \alpha_{ni} * S_n \quad (3.14)$$

To compute the new G_i needed for a particular new load bus demand S_n , when all other load buses' demand is held constant (to uphold the formulation and derivation principle, we adhere to a stepwise approach for the calculations), equation (3.14) is used. The new value of total generator output is deducted from the initial value of the total generator output to obtain the reserve capacity that a designated supply unit ought to have to meet the load demand.

For load capacity allocation, the load demand S_n from (3.14) is derived as

$$\alpha_{ni} * S_n = G_i - \sum_{k \neq n}^N \{ \alpha_{ki} * S_k \} \quad (3.15)$$

Dividing by α_{ni} , the following is attained

$$S_n = \frac{G_i}{\alpha_{ni}} - \frac{1}{\alpha_{ni}} \sum_{k \neq n}^N \{ \alpha_{ki} * S_k \} \quad (3.16)$$

To compute maximum load demand allocation, the rated output (or operational capacity available or slated for future connection) of the generator G_i is used. If this generator (or any specific supply unit) is set to offer reserve power, then the maximum permissible output is used to calculate the required maximum demand.

In power systems, inductive loads' massive demand for reactive power may lead to a severe voltage profile collapse [1]. Solutions to this collapse problem involve relieving the generator units from supplying reactive power to create more reserve capacity for real power [9]. That being so, there is the need to identify susceptible nodes for reactive power compensation [12] [30]. Voltage stability indices play an essential role in determining the system's critical buses and assessment studies about their similar relationship are crucial [13]. In section 3.4., a link between $\Delta V/\Delta Q$ self-sensitivities and the reduced Jacobian matrix was derived and presented.

3.4. Deriving $\Delta V/\Delta Q$ Self-sensitivities from Reduced Jacobian Matrix

Using the power flow Jacobian matrix

$$\begin{pmatrix} \Delta P \\ \Delta Q \end{pmatrix} = \begin{pmatrix} J_{11} & J_{12} \\ J_{21} & J_{22} \end{pmatrix} \begin{pmatrix} \Delta \theta \\ \Delta V \end{pmatrix} \quad (3.17)$$

Where: ΔP and ΔQ = mismatch active and reactive power vectors. ΔV and $\Delta \theta$ = unknown voltage magnitude and angle correction vectors. A relationship between $\Delta V/\Delta Q$ sensitivities and the reduced Jacobian matrix is found. It is well understood that the system voltage is affected by both real and reactive power variations [9] [40]. As a result, to focus on the study of reactive power demand and its supply problem in the system while reducing the computational effort, we let $\Delta P = 0$

$$\Delta P = 0 = J_{11} \Delta \theta + J_{12} \Delta V \quad (3.18)$$

Equation (3.18) becomes

$$\Delta \theta = - J_{11}^{-1} J_{12} \Delta V \quad (3.19)$$

From (3.17), we get

$$\Delta Q = J_{21} \Delta \theta + J_{22} \Delta V \quad (3.20)$$

Substituting (3.19) into (3.20), we have

$$\Delta Q = J_R \Delta V \quad (3.20a)$$

Where

$$J_R = J_{22} - J_{21} J_{11}^{-1} J_{12} \quad (3.20b)$$

Equation (3.20b) is the reduced Jacobian matrix [40]. That being so (3.20a) can be expressed as

$$\frac{\Delta V}{\Delta Q} = J_R^{-1} \quad (3.21)$$

Eigenvalue decomposition of J_R^{-1} is as follows

$$\frac{\Delta V}{\Delta Q} = \frac{\eta_i \mu_i}{\lambda_i} \quad (3.22)$$

Diagonal elements λ_i are the reduced Jacobian matrix eigenvalues and represent the $\Delta V/\Delta Q$ self-sensitivities.

3.5. Derivation of Multi-Bus V-Q curve Based Index

The analysis results of voltage stability in power systems are hugely determined by the reactive power of the system's load buses. The conventional way to ascertain critical voltage buses is typically done by subjecting the system to gradual reactive power changes at each load bus [11]. However, this approach is limited when the power system network is loaded simultaneously at multiple buses. The approach is limited because the sum effect of how buses are enmeshed influences the voltage profiles of load buses in a power system [15].

Assuming reactive power generation is adequate to supply load without violating the network's line limits, the load is varied across a range of reactive power (MVAR) for sole bus and multiple bus demands. Consequently, a new index is developed, considering the effect of uniformly distributed loading conditions on V-Q curve plot characteristics of a specific single/sole load bus.

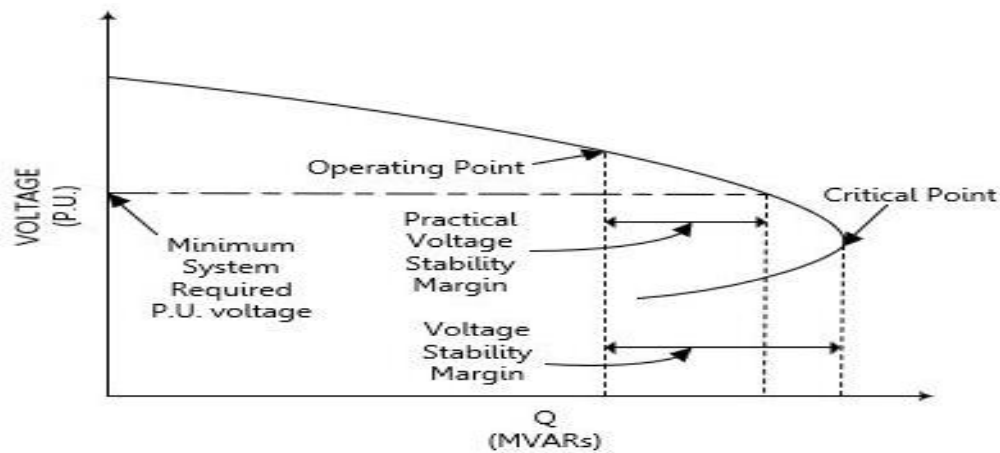


Figure 3.1: V-Q curve of a sole bus loading

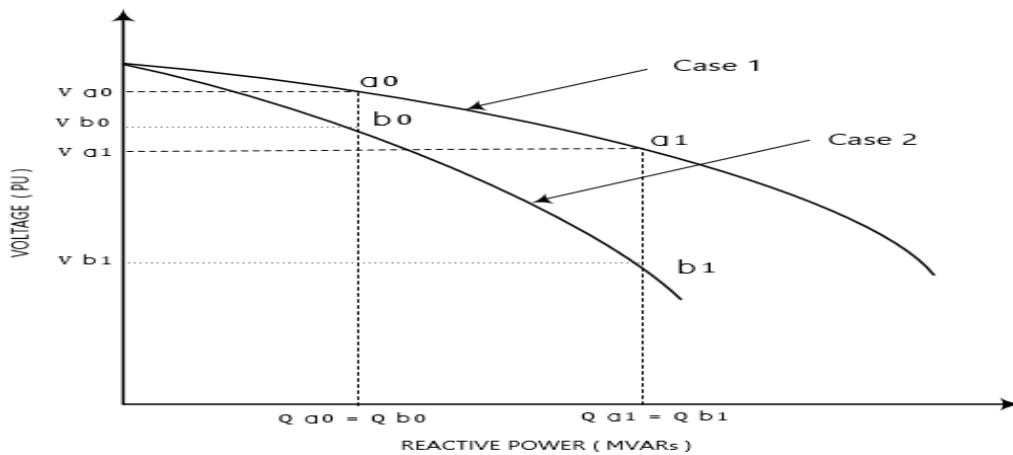


Figure 3.2: V-Q curve of a particular bus for sole bus loading and multi-bus loading

Figure 3.1 graphically presents the V-Q curve plot of a particular bus under investigation. From Figure 3.2, *case 1* represents sole or individual bus loading while *case 2* represents the multi-bus loading V-Q curve for a particular bus. V_{a0} and V_{a1} are points of the V-Q curve corresponding to Q_{a0} and Q_{a1} respectively. V_{b0} and V_{b1} are points of the V-Q curve corresponding to Q_{b0} and Q_{b1} respectively. The minimum allowable per unit voltage before the system collapse determines the choice of values V_{a1} and V_{b1} (they must be within the voltage stability region).

For case 1, let

$$\nabla_{case1} = \left| \frac{\Delta V_{case1}}{\Delta Q_{case1}} \right| = \left| \frac{V_{a0} - V_{a1}}{Q_{a0} - Q_{a1}} \right| \quad (3.23)$$

For case 2, let

$$\nabla_{case2} = \left| \frac{\Delta V_{case2}}{\Delta Q_{case2}} \right| = \left| \frac{V_{b0} - V_{b1}}{Q_{b0} - Q_{b1}} \right| \quad (3.24)$$

Then

$$\nabla_{total} = \nabla_{case1} - \nabla_{case2} \quad (3.25)$$

Which equates to

$$\nabla_{total} = \left| \frac{V_{a0} - V_{a1}}{Q_{a0} - Q_{a1}} \right| - \left| \frac{V_{b0} - V_{b1}}{Q_{b0} - Q_{b1}} \right| \quad (3.25a)$$

Thus, the proposed Voltage Critical Multi-Bus Index (VCMBI) is formulated as follows

$$\text{VCMBI} = |\nabla_{total}| \quad (3.26)$$

$$\text{VCMBI} = \left| \left| \frac{V_{a0} - V_{a1}}{Q_{a0} - Q_{a1}} \right| - \left| \frac{V_{b0} - V_{b1}}{Q_{b0} - Q_{b1}} \right| \right| \quad (3.27)$$

3.6. Conclusion

Using one of the ISTN indices (the ideal generator contribution index), a method of allocating generator reserves (as well as required additional capacity) and maximum permissible load demand (at a particular bus) was developed. Also, an index to investigate the real strength of a specific bus, the effect of multiple bus loading on the particular chosen bus's voltage magnitude, has been derived. The magnitude of the slope indicates susceptibility to voltage collapse. Therefore, the bus with the highest magnitude (after calculating the difference between single loading stiffness and multiple bus loading stiffness) is the most susceptible to voltage collapse at the particular reactive power loadings.

CHAPTER 4 – SIMULATIONS AND RESULTS

4.1. Introduction

The generator reserve and load capacity allocation using the ideal generator contribution index results are presented in section 4.3. The MATLAB software was used to code the ISTN's indices for both test systems (Appendix A). Section 4.4 represents the voltage stability index based on multi-bus reactive power loading. Power World simulator and Dig SILENT Power Factory software were used for simulating the Southern Indian Network and the IEEE 14 bus systems respectively (Appendix B). Line data for the systems is also found in Appendix B. MATLAB software was used for the voltage critical multi-bus index graphical data presentation. $V-Q$ curves plots for the single bus loading are shown for buses 5 and 6 in Southern Indian Network, with all other load buses graphs presented in Appendix C. A general illustration and classification of voltage stability indices for comparison is showcased in Appendix D.

4.2. Test System Models

The Equivalent Southern Indian Network, the IEEE 14 bus system and its modified case are shown below (Figures 4.1, 4.2 and 4.3). For the modified case, the IEEE 14 bus system bus numbering is re-arranged to represent sources first (generators) and then sink (load) buses respectively in ascending order from bus 1 to 14. This bus re-numbering is essential in most systems and it is the only significant alteration done to any system under investigation. In the case of a bus with both source and sink, it is essential to note that the power injection of the bus determines the classification of that particular bus (based on whether it is sourcing or sinking power) at the instance of system investigation. In our case, we have taken all generators and compensators as sources (generators for either real power or reactive power) only.

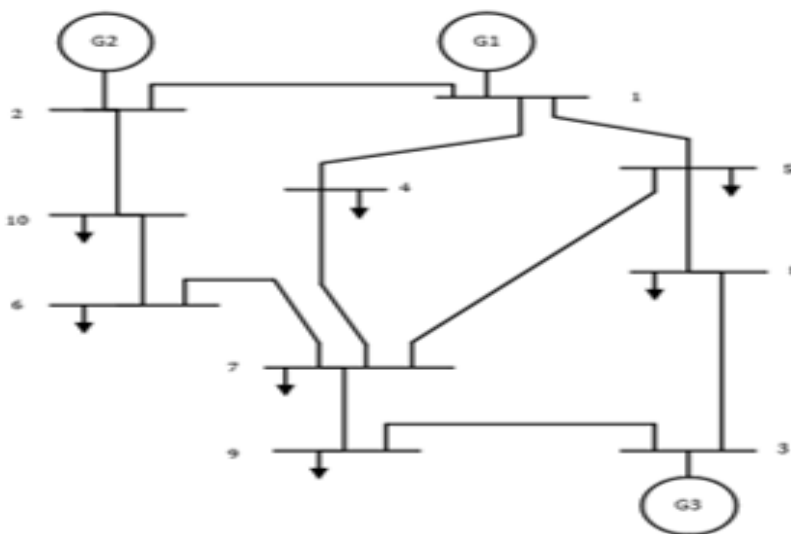


Figure 4.1: Equivalent Southern Indian Network [18].

4.3. Simulation and Results for Generator Reserve and Load Capacity Allocation Using Ideal Generator Contribution

4.3.1. Case Study 1: 10 Bus Southern Indian Network

For the Southern Indian Network, graphical results from Figures 4.4 and 4.5 show that in overall power requirements, both sole and uniformly distributed load bus demand exerts similar pressure on specific units when it comes to power supply. It is worth noting that the load buses have been subjected to reactive power demand, which is usually absorbed by most electrical machines in industries and urban located premises. G_3 supplies most of the power; hence its location is most suited for a baseload power plant in this particular power network.

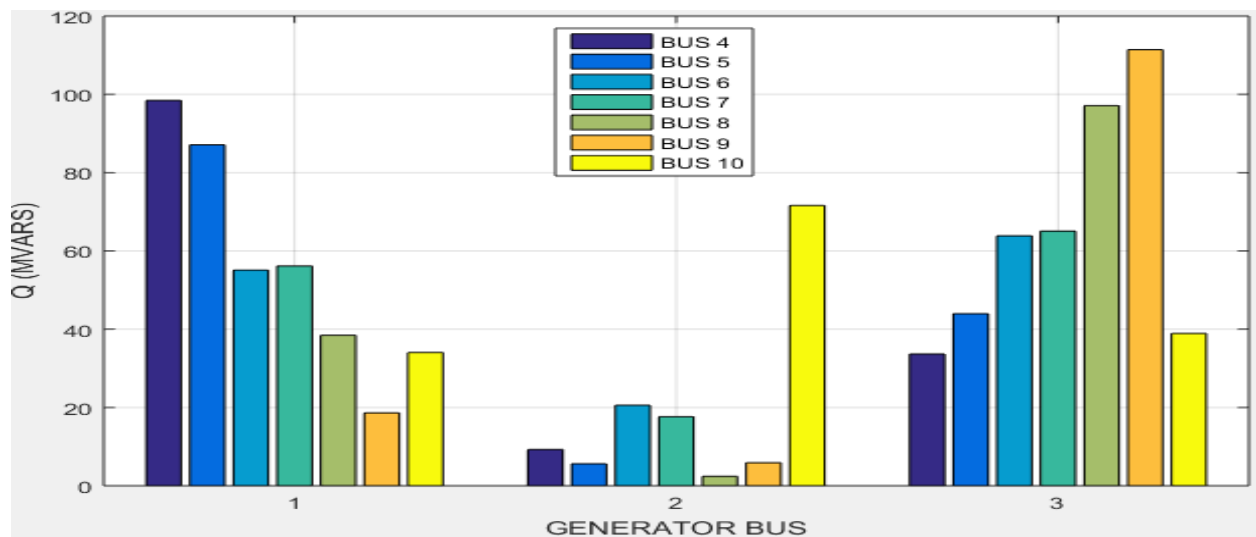


Figure 4.4: Graphical representation of generator power contribution to meet sole bus load demand in Southern Indian Network using MATLAB software.

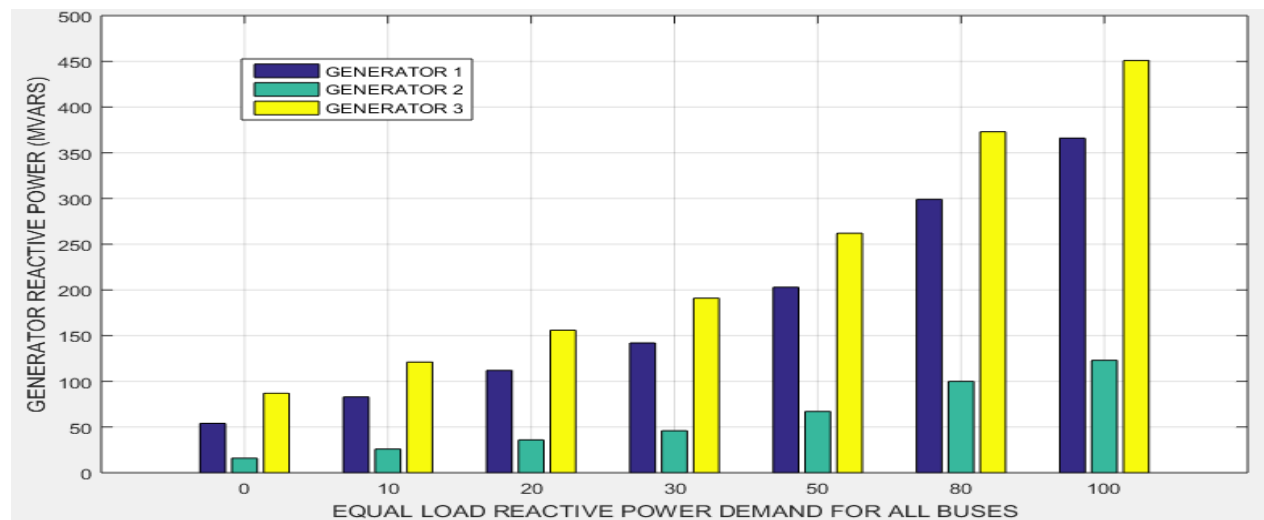


Figure 4.5: Graphical representation of generator power contribution to meet uniformly distributed multi-bus load demand in Southern Indian Network using MATLAB software.

In the results, Tables 4.1 and 4.5 present the ideal generator contribution index results for both systems under investigation. From the tabulated results, it is worth noting that a generator with much share of electrical loads typically takes an index value more significant than the rest. Table 4.2 shows the load demand (MW) and generation schedule for the base load case in Southern Indian Network System, while Table 4.3 presents the simulated results from the power world simulator. In the ideal generator contribution index, the power is allocated to generator units similarly when either (real or reactive) power is considered (as shown in Table 4.3, in Figures 4.3 and 4.5).

Table 4.1: Ideal Generator Contribution for Southern Indian Network, $|F_{LG}|$

Load Bus Number	Generator Bus		
	G1	G2	G3
L4	0.7020	0.0637	0.2344
L5	0.6414	0.0395	0.3191
L6	0.3947	0.1483	0.4570
L7	0.4045	0.1273	0.4683
L8	0.2783	0.0172	0.7045
L9	0.1348	0.0424	0.8227
L10	0.2294	0.5051	0.2655

Table 4.2: Load Demand and Generation Schedule for Base Load Case, Southern Indian Network [22]

Load Bus Number	Load (MW)	Generator Bus		
		G1	G2	G3
L4	100	71.0	6.5	23.9
L5	150	96.9	6.0	48.8
L6	180	70.9	27.1	83.3
L7	250	102.8	32.8	120.5
L8	320	89.7	5.6	228.8
L9	300	40.6	12.9	249.9
L10	50	11.5	25.6	13.5
Total generation (MW)		483.4	116.5	768.7

Table 4.3: Simulation Results Showing Base Case Load-Supply in Southern Indian Network using Power World Simulator

	Load (MW)	Load (MVAR)	Gen (MW)	Gen (MVAR)
G1			483.40	635.56
G2			116.66	157.16
G3			786.84	993.57
L4	100	100		
L5	150	150		
L6	180	180		
L7	250	250		
L8	320	320		
L9	300	300		
L10	50	50		

Table 4.4 shows the load power demand and the corresponding generation schedule when the load at bus 7 increases from 250 MW to 350 MW in the Southern Indian Network. The total power generation designated for production by a particular unit is calculated using the equation (3.14). G_1 is shown to increase its supply by 39 MW, G_2 by 11.75 MW and G_3 by 43.4 MW. From the analysis of the results, it befits the power system operators and designers to slate a minimum reserve capacity of 39 MW, 11.75 MW and 43.4 MW for generators G_1 , G_2 and G_3 respectively. This method of reserve allocation is subject to the merits of using the ideal generator contribution index as discussed in chapters 2 and 3. The simulated results of Table 4.4 are shown in Table 4.6. The error margins between calculated results and the simulated results are 0.226 MW, -0.003 MW and 3.488 MW for generators G_1 , G_2 and G_3 respectively.

Table 4.4: Load Demand and Generation Schedule When Bus 7 Load Demand Is Projected To 350 MW, In Southern Indian Network

Load Bus Number	Load Value (MW)	Generator Bus		
		G1	G2	G3
L4	100	71.0	6.5	23.9
L5	150	96.9	6.0	48.8
L6	180	70.9	27.1	83.3
L7	350	141.575	44.555	163.905
L8	320	89.7	5.6	228.8
L9	300	40.6	12.9	249.9
L10	50	11.5	25.6	13.5
Total generation (MW)		522.175	128.255	812.105

Table 4.5: Ideal Generator Contribution for IEEE 14 Bus System, $|F_{LG}|$

Load Bus Number	Generator Bus				
	G1	G2	G3	G4	G5
L6	0.1148	0.3745	0.2331	0.1691	0.1090
L7	0.0515	0.1679	0.1045	0.2230	0.4633
L8	0.1889	0.3788	0.1434	0.2189	0.0671
L9	0.0492	0.1605	0.0999	0.3924	0.3187
L10	0.0407	0.1327	0.0826	0.4972	0.2634
L11	0.0209	0.0681	0.0424	0.7412	0.1353
L12	0.0036	0.0116	0.0072	0.9553	0.0230
L13	0.0071	0.0233	0.0145	0.9114	0.0463
L14	0.0309	0.1008	0.0627	0.6165	0.2002

Table 4.6: Simulation Results Showing Load-Supply For Bus 7 At 350 (MW) In Southern Indian Network Using Power World Simulator

	Load (MW)	Load (MVAR)	Gen (MW)	Gen (MVAR)
G1			522.40	66.96
G2			128.25	20.07
G3			815.59	104.45
L4	100	0.00		
L5	150	0.00		
L6	180	0.00		
L7	350	0.00		
L8	320	0.00		
L9	300	0.00		
L10	50	0.00		

Table 4.7 presents permissible load demand at bus 5 in the same system when G_2 is restricted to a maximum power supply of 120 MW. The calculated results give a value of 240.5 MW from 150 MW for bus 5. That being so, G_1 generates 57.35 MW as additional power while G_3 is apportioned to supply 27.94 MW extra power (reserve power). The simulated results are shown in Table 4.8. There is a 0.25 MW margin from calculated results.

Table 4.7: Permissible Load Demand at Bus 5 and Generation Schedule When Generator 2 Maximum Supply Is 120 MW, In Southern Indian Network

Load Bus Number	Load Value (MW)	Generator Bus		
		G1	G2	G3
L4	100	71.0	6.5	23.9
L5	240.5	154.25	9.48	76.74
L6	180	70.9	27.1	83.3
L7	250	102.8	32.8	120.5
L8	320	89.7	5.6	228.8
L9	300	40.6	12.9	249.9
L10	50	11.5	25.6	13.5
Total generation (MW)		540.75	120.0	796.64

Table 4.8: Simulation Results Showing Permissible Load Capacity at Bus 5, When Supply from Generator 2 is Set Maximum at 120 (MW), in Southern Indian Network Using Power World Simulator.

	Load (MW)	Load (MVAR)	Gen (MW)	Gen (MVAR)
G1			540.40	63.82
G2			120.25	16.82
G3			794.85	95.22
L4	100	0.00		
L5	240	0.00		
L6	180	0.00		
L7	250	0.00		
L8	320	0.00		
L9	300	0.00		
L10	50	0.00		

4.3.2. Case Study 2: The Modified IEEE 14 Bus System

In the modified IEEE 14 Bus System, figures 4.6 and 4.7 prove that the generator located at bus 4 supplies most of the power needed to meet load demand for sole bus loading and uniformly distributed multi-bus loading. Figure 4-8 shows that a particular system network normally absorbs reactive power even when no loading is applied; thus, generating reactive power is done to cater to both system and load requirements. G_4 ability to absorb excess power is essential in maintaining operational voltage limits in cases related to the receiving end of long transmission lines. It is worth noting that both supply sources and demand sinks must be connected to the system to simulate the behavior of source and sink buses properly.

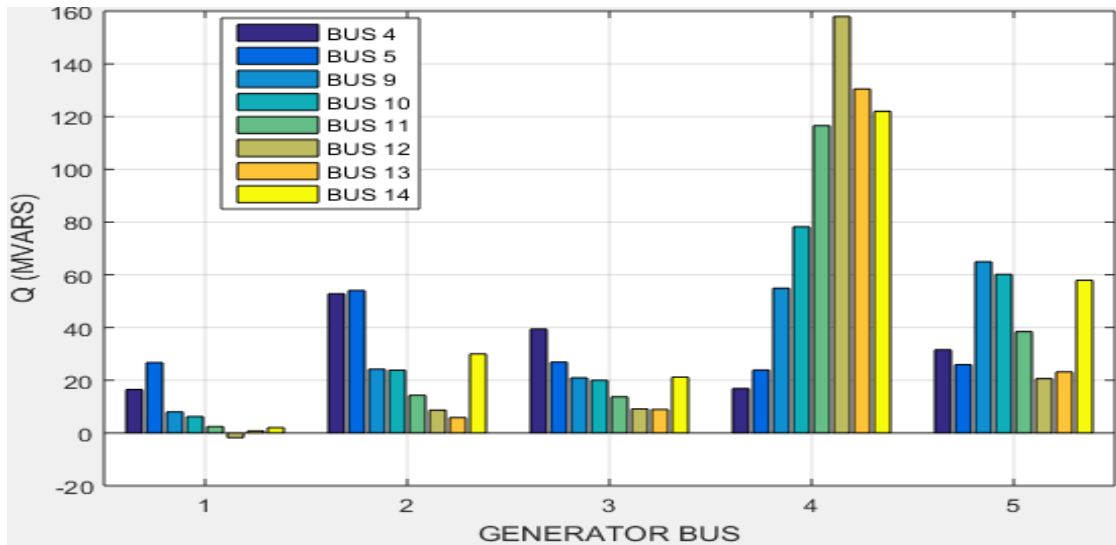


Figure 4.6: Generator power contribution to meet sole bus load demand in the modified IEEE 14 Bus System.

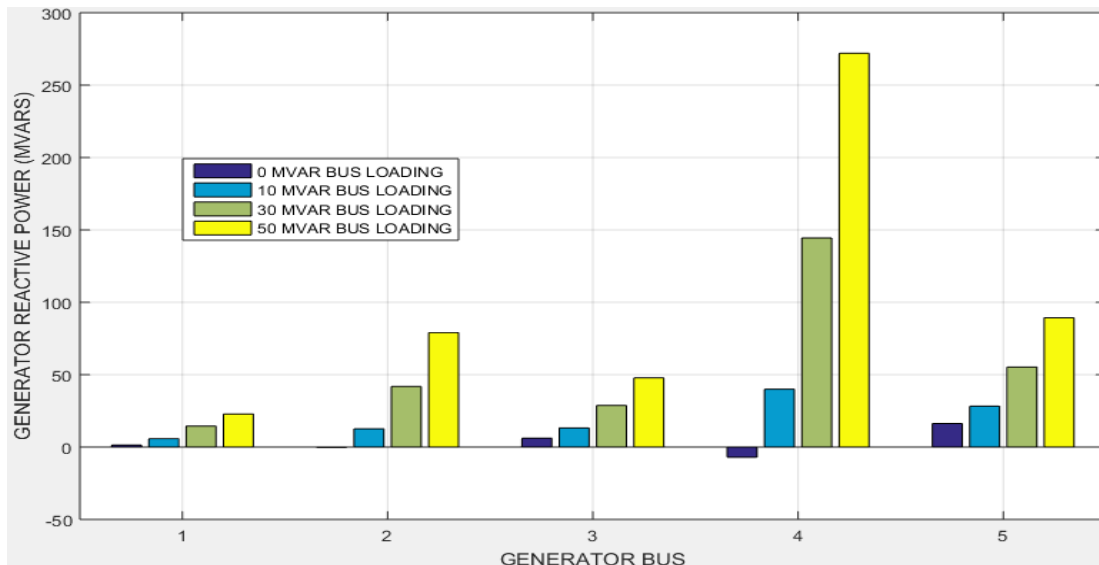


Figure 4.7: Generator power contribution to meet uniformly distributed multi-bus load demand in the modified IEEE 14 Bus System.

The generators' reactive power contributions presented below include the entire network's power required to keep the system in stable operation.

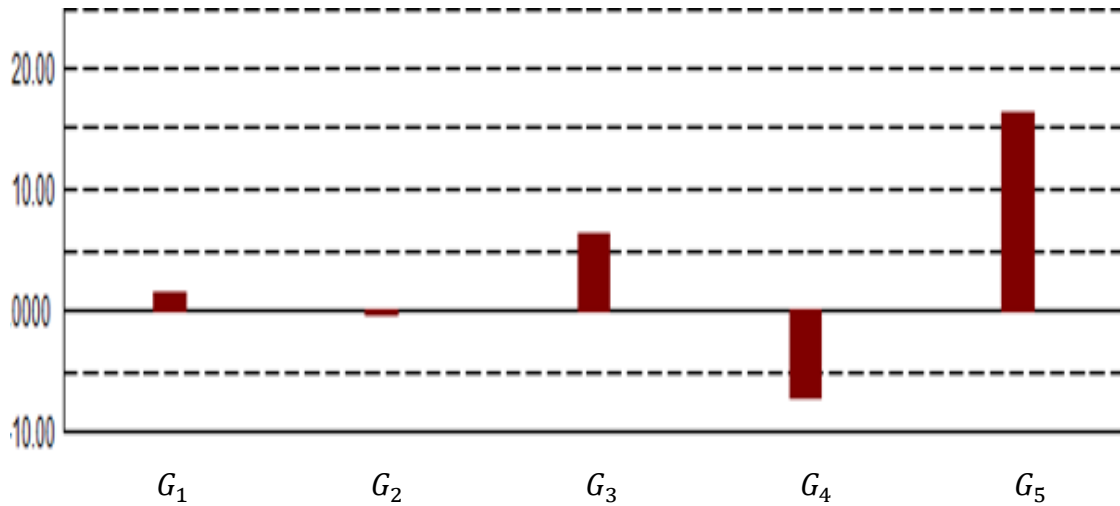


Figure 4.8: Results showing generator contribution to meet network's reactive power demand in IEEE 14 Bus System using Dig-SILENT Power Factory.

In the modified IEEE 14 Bus System, the simulated results are generated graphically and presented in figure form. For Figures: 4.8, 4.9, 4.10 and 4.11. Figure 4.9 presents the power supply (MW) for the base-case load. Figure 4.10 shows power supply (MW) when power demand is 20 (MW) at load bus 8, Figure 4.11 shows power supply (MW) for all generator units when G_4 is set to a maximum output of 52 (MW) for permissible load capacity investigation in load bus 12. The magnitudes of real power (MW) were selected randomly but within reasonable ranges. The corresponding calculated values of Figures 4.9, 4.10 and 4.11 are presented in Table 4.9, 4.10 and 4.11, respectively.

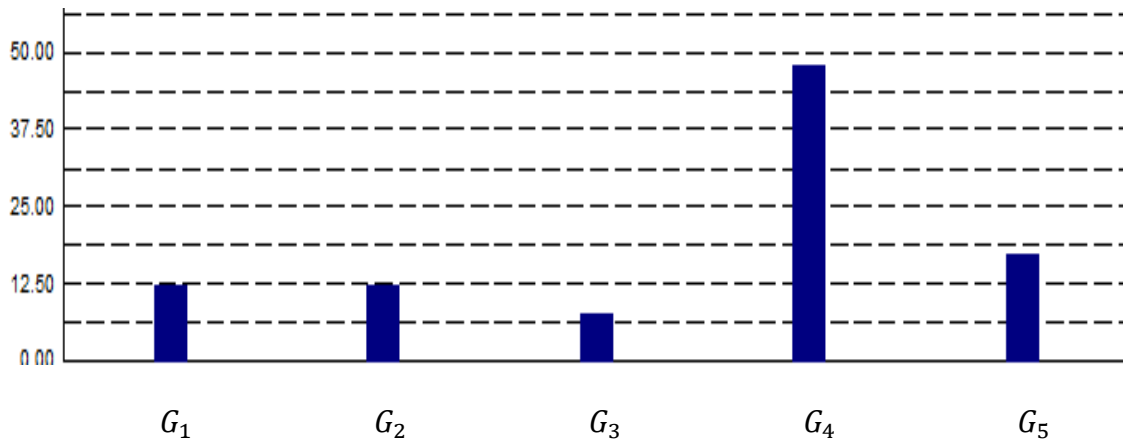


Figure 4.9: Results showing base case load-supply in the modified IEEE 14 Bus System using Dig-SILENT Power Factory.

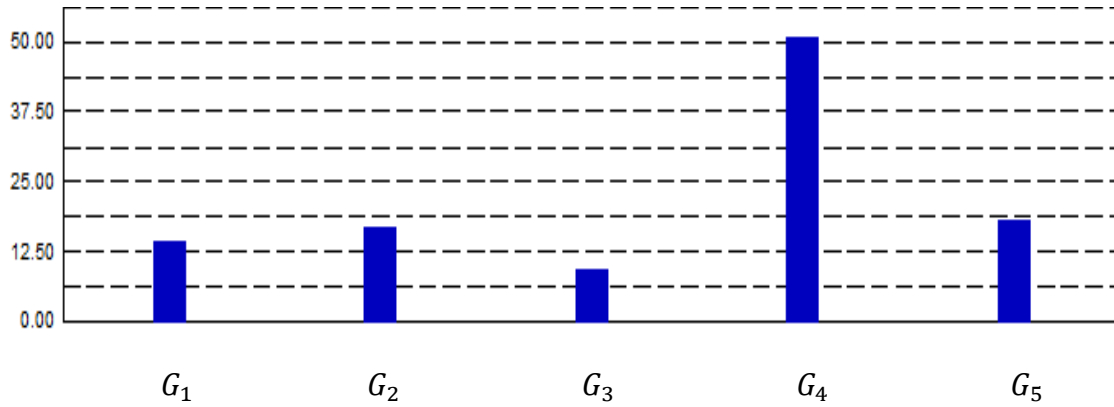


Figure 4.10: Results showing load-supply when bus 8 is at 20 MW, in the modified IEEE 14 Bus System, using Dig-SILENT Power Factory.

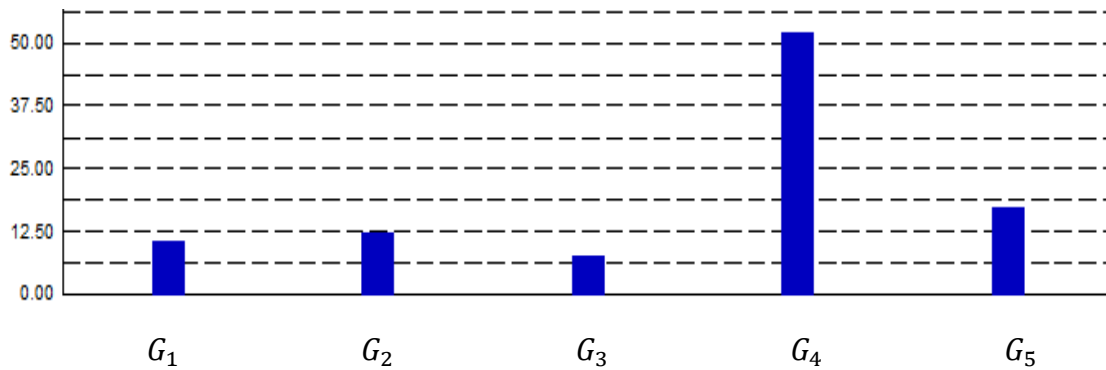


Figure 4.11: Results showing the power supply for all units when Generator 4 is set the maximum at 52 (MW), in the modified IEEE Bus System using Dig-SILENT Power Factory.

Table 4.9: Load Data and Generation Schedule for Base Load Case, in the modified IEEE 14 Bus System Using Ideal Generator Contribution Index

Load Bus Number	Base Load Value (MW)	Generator Bus				
		G1	G2	G3	G4	G5
L6	11.2	1.285	4.194	2.610	1.894	1.221
L7	Node	-				
L8	7.6	1.435	2.878	1.089	1.663	0.509
L9	29.5	1.451	4.734	2.947	11.575	9.402
L10	9	0.366	1.194	0.743	4.474	2.371
L11	3.5	0.073	0.238	0.148	2.594	0.473
L12	6.1	0.022	0.070	0.044	5.827	0.140
L13	13.5	0.096	0.314	0.195	12.303	0.625
L14	14.9	0.460	1.502	0.934	9.185	2.982
Total generation		5.188	15.124	8.710	49.515	17.723

For G_3 , G_4 and G_5 , the simulated and calculated power (MW) magnitudes are approximately similar (in other terms, the values are in great harmony), as seen from the presented results above. For G_1 , simulated power is 7.312 MW greater than the calculated value while for G_2 the simulated value is 2.624 MW lesser than the ideal calculated value. With G_1 being the slack bus, this difference in power (MW) can be understood to meet the overall system losses (apart from load power demand in MW).

When bus 8 load demand is projected to 20 MW from 7.6 MW, G_2 contributes most to power requirements of the new load demand as deduced from simulated and calculated results in Figure 4.10 and Table 4.10, respectively. This makes this generator the best-suited place for reserve allocation. In Table 4.11, the permissible load demand at bus 12 and generation schedule when G_4 maximum supply is 52 MW. It is pretty evident that a generator's output power limit can be used to determine the maximum power demand (load placement) chosen for a particular bus using the ideal generator contribution index.

Table 4.10: Load Data and Generation Schedule when Bus 8 Load Demand is Projected to 20 MW In the modified IEEE 14 Bus System

Load Bus Number	Load Value (MW)	Generator Bus				
		G1	G2	G3	G4	G5
L6	11.2	1.285	4.194	2.610	1.894	1.221
L7	Node	-				
L8	20	3.778	7.576	2.868	4.378	1.342
L9	29.5	1.451	4.734	2.947	11.575	9.401
L10	9	0.366	1.194	0.743	4.474	2.371
L11	3.5	0.073	0.238	0.148	2.594	0.474
L12	6.1	0.022	0.070	0.044	5.827	0.140
L13	13.5	0.096	0.315	0.195	12.303	0.625
L14	14.9	0.460	1.502	0.934	9.186	2.983
Total generation		7.531	19.823	10.489	52.231	18.557

Table 4.11: Permissible Load Demand at Bus 12 and Generation Schedule when Generator 4 Maximum Supply is 52 MW In the modified IEEE 14 Bus System

Load Bus Number	Load Value (MW)	Generator Bus				
		G1	G2	G3	G4	G5
L6	11.2	1.285	4.194	2.610	1.894	1.221
L7	Node	-				
L8	7.6	1.435	2.878	1.089	1.663	0.509
L9	29.5	1.451	4.734	2.947	11.575	9.402
L10	9	0.366	1.194	0.743	4.474	2.371
L11	3.5	0.073	0.238	0.148	2.594	0.474
L12	8.703	0.031	0.101	0.063	8.314	0.200
L13	13.5	0.096	0.315	0.195	12.303	0.625
L14	14.9	0.460	1.502	0.934	9.186	2.983
Total generation		5.197	15.156	8.729	52.003	17.785

4.4. Simulation and Results for Voltage Stability Index Based on Multi-bus Reactive Power Loading

4.4.1. Case Study 1: 10 Bus Southern Indian Network

Figures 4.12 and 4.13 show the influence of load buses 5 and 6 (in Southern Indian Network) on other buses' voltage profiles respectively. In Figure 4.12, Bus 5 sole loading has a large effect on the voltage drop of Bus 8 as compared to the sole loading of Bus 6. This proves that a particular bus MVARs loading usually affects other buses voltage profiles (in different magnitudes) and therefore, this phenomenon must be taken into account during real-time application of voltage stability analysis.

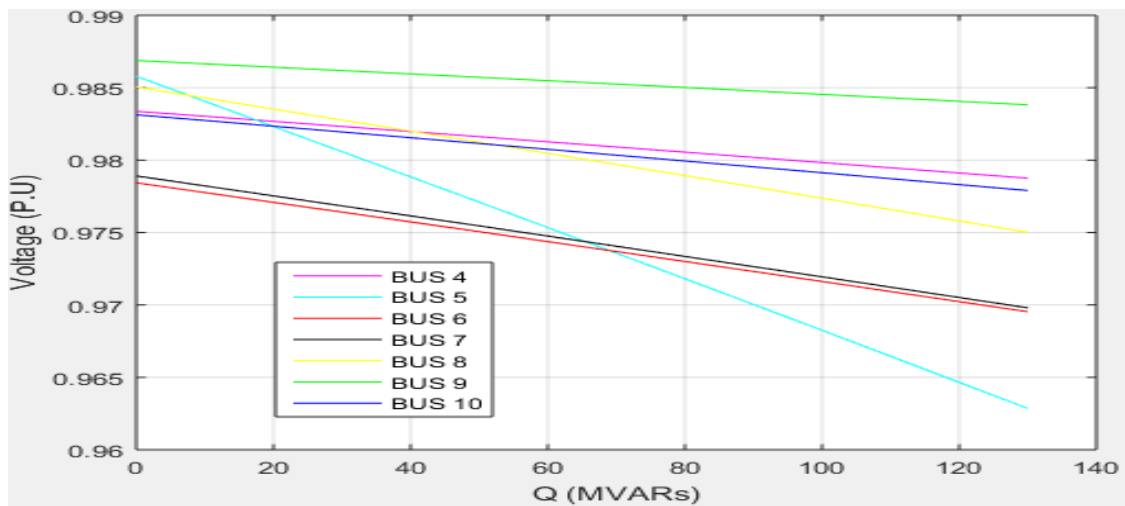


Figure 4.12: V-Q curves comparison for all load buses when only bus 5 is loaded at Southern Indian Network System

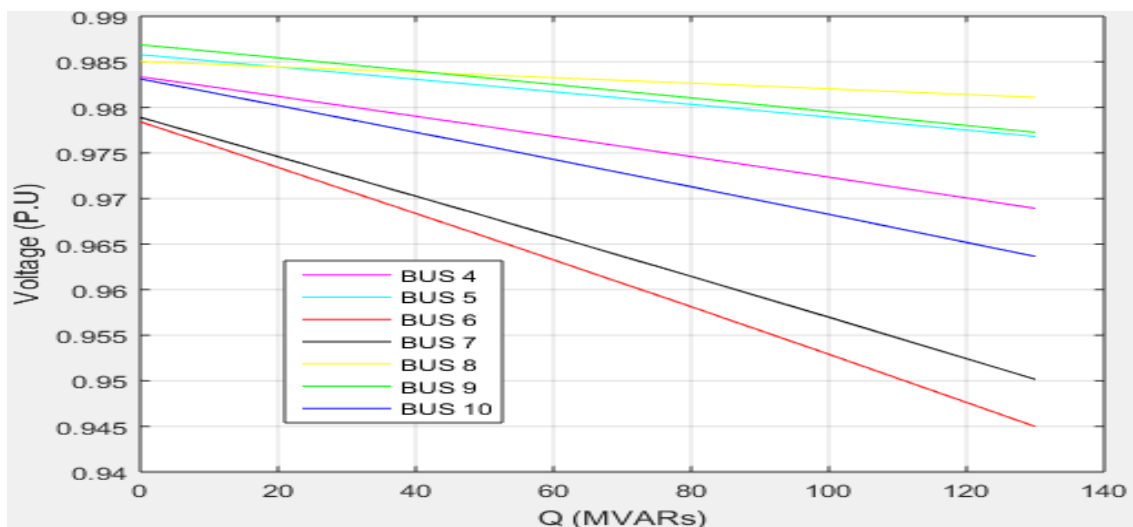


Figure 4.13: V-Q curves comparison for all load buses when only bus 6 is loaded at Southern Indian Network System

Figure 4.14 demonstrates the relationship between V-Q curves when each bus is loaded at a time. Bus 10 suffers the most voltage drop (per MVARs variation) compared to all the other load buses and Bus 9 experiences the least voltage drop. Figure 4.15 demonstrates how the same systems subjected to voltage stability investigation usually have their V-Q curve plots under uniform load applied simultaneously on load buses. This incorporates the mutual effects of each bus as voltage sag is concerned. Bus 6 suffers the most voltage drop (per MVARs variation) and can be deemed as the weakest bus in this context.

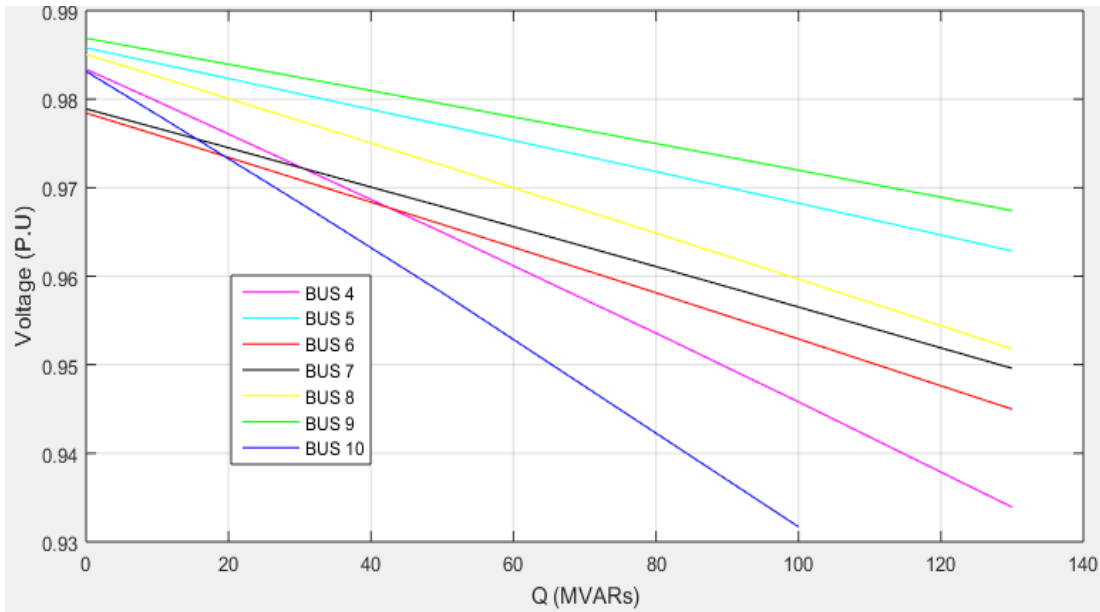


Figure 4.14: V-Q curves comparison for Southern Indian Network System when all buses are loaded at a time

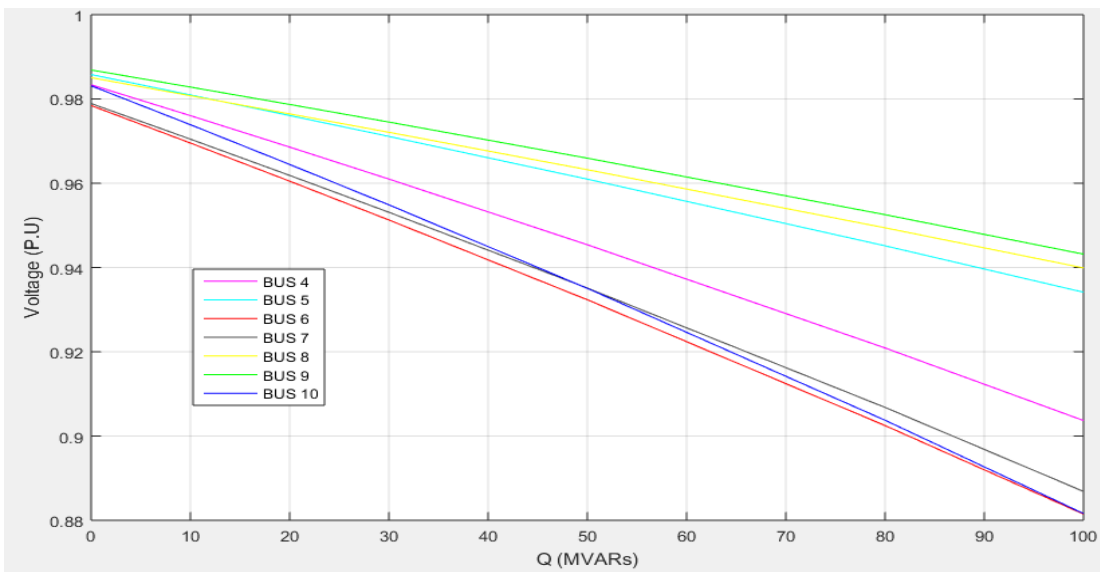


Figure 4.15: V-Q curves comparison for Southern Indian Network System when all buses are loaded simultaneously and uniformly

Table 4.12 shows the eigenvalue analysis of the networks' load structural electrical attraction regions using the Y -admittance matrix partitioning approach [15]. This captures the inherent characteristics of the system network without the effect of very adverse loading conditions. The eigenvalues help identify the weak nodes and buses from the system's structure which is reasonably accurate for most uniform and practical light-load conditions of an interconnected network operation. The ranking of load buses begins with the weakest bus to the strongest bus in ascending order.

Table 4.12: Load Structural Electrical Attraction Region for the Southern Indian Network [15]

Load Bus Number	Eigenvalue	Ranking
L4	540.5241	7 th
L5	80.6565	6 th
L6	0.0014	1 st
L7	56.6405	5 th
L8	40.9676	4 th
L9	27.5772	3 rd
L10	20.0941	2 nd

Table 4.13 demonstrates the V - Q self-sensitivities of the systems under investigation. All eigenvalues are above zero, indicating the power system is voltage stable [13]. The ranking of load buses begins with the weakest bus to the strongest bus in ascending order. The results show that bus 5 is the weakest bus in the Southern Indian Network system.

Table 4.13: Eigenvalues of $\Delta V/\Delta Q$ Self-Sensitivities Using the Reduced Jacobian Matrix for Southern Indian Network System

Load Bus Number	Eigenvalue	Ranking
L4	477.7804	7 th
L5	10.6666	1 st
L6	24.3853	2 nd
L7	31.2385	3 rd
L8	40.3195	4 th
L9	83.4581	6 th
L10	76.6731	5 th

Table 4.14: VCMBI for the Southern Indian Network System

Load Bus Number	V_{case1}	V_{case2}	V_{total}	VCMBI	Ranking
Bus 4	0.036975	0.076600	-0.039625	0.039625	5 th
Bus 5	0.017400	0.049975	-0.032575	0.032575	6 th
Bus 6	0.025250	0.093000	-0.067750	0.067750	1 st
Bus 7	0.022175	0.088350	-0.066175	0.066175	2 nd
Bus 8	0.025100	0.043900	-0.047000	0.047000	3 rd
Bus 9	0.014825	0.042175	-0.027350	0.027350	7 th
Bus 10	0.050250	0.097100	-0.046850	0.046850	4 th

Table 4.14 presents Voltage Critical Multi-Bus Index results for Southern Indian Network System. A comparison is made between the new index (VCMBI) and the ISTN index (the load structural, electrical attraction region index). For the Southern Indian System, bus 6 has been identified as the weakest bus using both VCMBI and the load structural, electrical attraction region index. Buses 5 and 4 are in the pool of the strongest buses as presented by both indices. This can be ascribed to the relative electrical proximity between load centers and generator stations [22] [25].

4.4.2. Case Study 2: IEEE 14 Bus System

Figures 4.16 demonstrate the relationship between V-Q curves when each bus is loaded at a time. Bus 14 suffers the most voltage drop and Bus 7 has the least voltage deviation in the range of 0-120 MVARs. Figure 4.17 demonstrates how the same systems subjected to voltage stability investigation usually have their V-Q curve plots under even load applied across all load buses simultaneously. Buses 14, 10 and 9 have the most voltage deviation and can be termed as the weakest buses in this context. This V-Q curve plot incorporates the mutual effects of each bus as voltage sag is concerned.

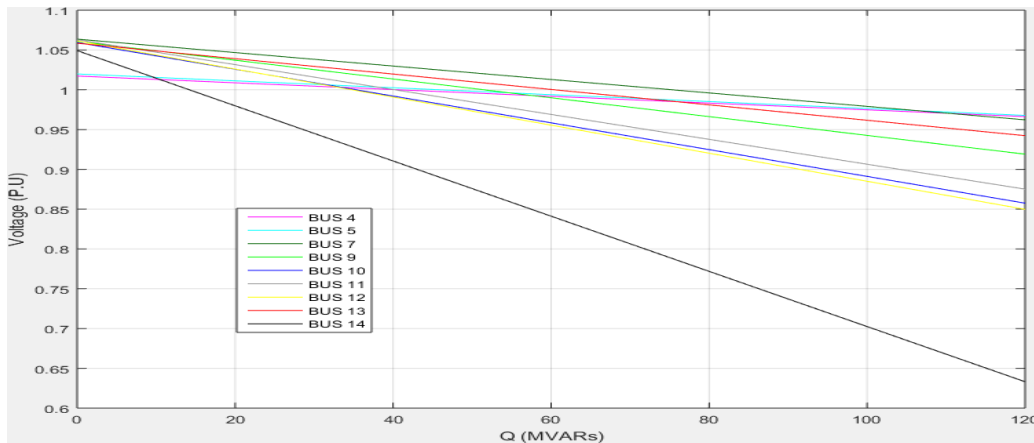


Figure 4.16: V-Q curves comparison for IEEE 14 bus system when each bus is loaded individually at a time

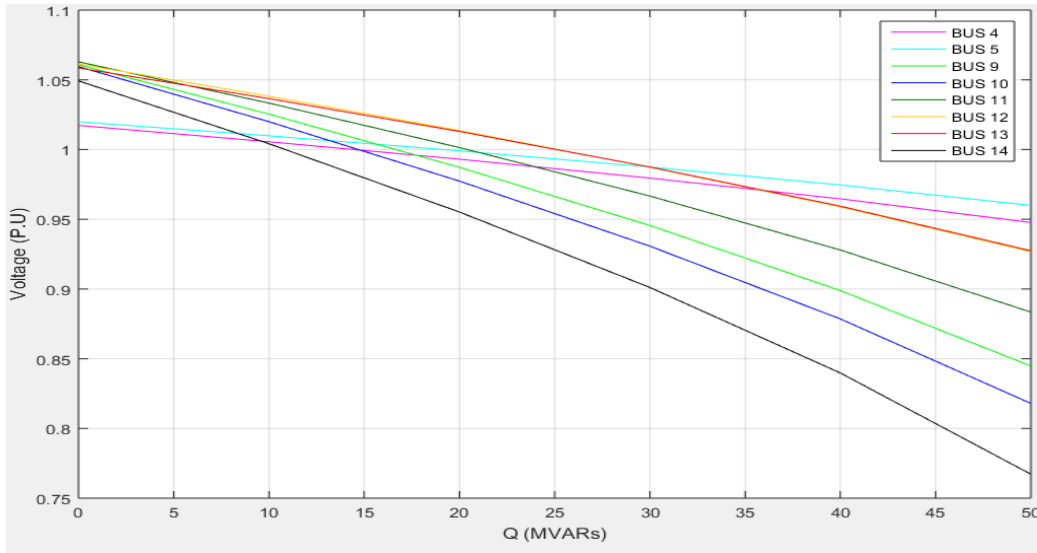


Figure 4.17: V-Q curves comparison for IEEE 14 bus system when all buses are loaded simultaneously and uniformly

Table 4.15 show the eigenvalue analysis of the networks' load structural electrical attraction regions using the Y -admittance matrix partitioning approach [15]. They capture the inherent characteristics of the system network without the effect of very adverse loading conditions. The eigenvalues help identify the weak nodes and buses from the system's structure which is reasonably accurate for most uniform and practical light-load conditions of an interconnected network operation. The ranking of load buses begins with the weakest bus to the strongest bus in ascending order.

Table 4.15: Load Structural Electrical Attraction Region for IEEE 14 Bus System

Load Bus Number	Eigenvalue	Ranking
L4	59.0441	9 th
L5	16.3948	8 th
Bus/Node 7	34.5780	7 th
L9	13.6334	6 th
L10	0.0278	1 st
L11	9.8076	5 th
L12	3.4409	2 nd
L13	5.3466	3 rd
L14	5.7002	4 th

Table 4.16 demonstrates the V-Q self-sensitivities of the systems under investigation. All eigenvalues are above zero, indicating the power system is voltage stable. The ranking of load buses begins with the weakest bus to the strongest bus in ascending order. Bus 11 is the weakest load bus, and bus 4 is the strongest.

Table 4.16: Eigenvalues of $\Delta V/\Delta Q$ Self-Sensitivities Using the Reduced Jacobian Matrix for IEEE 14 Bus Network System

Load Bus Number	Eigenvalue	Ranking
L4	36.8457	9 th
L5	20.1539	7 th
L7	26.1558	8 th
L9	15.3775	6 th
L10	11.0254	5 th
L11	0.8158	1 st
L12	2.5802	2 nd
L13	5.7255	4 th
L14	4.9108	3 rd

Table 4.17 presents the Voltage Critical Multi-Bus Index (VCMBI) results in IEEE 14 Bus System. A comparison is made between the new index (VCMBI) and the ISTN index (the load structural, electrical attraction region index). For IEEE 14 bus System, bus 10 is identified as the weakest bus for the two indices. The buses with both source and sink (loads and generators) have not been included (in the load buses category) since they are constantly supplied at nominal voltage under normal operating system conditions using controller systems. Bus node 7 is unloaded, thus not presented for VCMBI in this case. From the analysis of results, buses 4 and 5 are the strongest as shown by the two indices and bus 10 is the weakest among all buses.

Table 4.17: VCMBI for the IEEE 14 Bus Network System

Load Bus Number	∇_{case1}	∇_{case2}	∇_{total}	VCMBI	Ranking
Bus 4	0.040905	0.1301760	-0.0892710	0.0892710	7 th
Bus 5	0.041780	0.1117745	-0.0699945	0.0699945	8 th
Bus 9	0.106275	0.3994535	-0.2931785	0.2931785	3 rd
Bus 10	0.142820	0.4462785	-0.3034585	0.3034585	1 st
Bus 11	0.134090	0.3331310	-0.1990410	0.1990410	4 th
Bus 12	0.145075	0.2546220	-0.1095470	0.1095470	6 th
Bus 13	0.088185	0.2450925	-0.1569075	0.1569075	5 th
Bus 14	0.221199	0.5154240	-0.2942245	0.2942245	2 nd

CHAPTER 5 – CONCLUSION AND RECOMMENDATIONS

5.1. Conclusion

Generator reserve allocation using the ideal generator contribution index has been effectively demonstrated. The generator slated to offer reserve power is the unit with the highest value of ‘ideal power contribution’ to meet a specific anticipated load demand in a particular bus. In a power system with increasing electrical power needs, the generator bus generally associated with high power contribution to the system demands is the best network’s node for additional siting of units. That being so, In Southern Indian Network and the modified IEEE 14 Bus System, bus 3 and bus 4 qualify as the best nodes for additional power supply units and reserve allocation respectively.

Load capacity allocation, which designates the maximum load permissible for a particular load bus (which depends on generation and transmission restrictions, i.e. permissible thermal limits), has been presented. Both systems under investigation show that much capacity for electrical load growth is feasible for a bus in close electrical proximity (from relative electrical distance, RED) to the high rated power output units.

The use and application of indices determine a piece of essential information regarding a power system. Practically, load centers are mainly distributed among the load buses and the power demand varies over time. That being so, the short-term and long-term matching of power demand and supply in a system is crucial. The Voltage Critical Multi-Bus Index has been derived and studied. Identifying the critical bus in a network was achieved by incorporating the mutual influence (on voltage and reactive power) that load buses have in an interconnected system at any instance of reactive load demand. The application of this index can aid significantly in the best operation of the network. This novel index determines, with precision, the nodes and buses which require the placement of reactive power compensators to meet reactive power demand in a power system.

5.2. Recommendation for Future Work

Implementing the voltage critical multi-bus index calculations in the power system’s simulation software is of necessity in determining the critical buses at any particular instances of multi-bus loading. The amount of reactive compensation can also be computed by further analysis of the resultant $V-Q$ curves plots of the multi-bus loading conditions. Also, incorporating the ideal generator contribution index (for generator reserve and load capacity allocation) in power design and planning software is an insightful approach (aimed at minimizing losses and network reconfiguration) for the interconnected power system networks.

REFERENCES

- [1] Steven W. Blume, “Interconnected Power Systems,” in *Electric Power System Basics for the Nonelectrical Professional*, John Wiley & Sons, Inc, 2017, pp. 165-186.
- [2] Jianxue Wang, Xifan Wang and Yang Wu, “Operating Reserve Model in the Power Market,” *IEEE Transactions on Power Systems*, vol. 20, no. 1, pp. 223-229, Feb. 2005.
- [3] Ivan Pavic, Matea Filipovic, Igor Kuzle and Yong-qian Liu, “Operating Reserve Allocation Methods Relative to Energy Unit Commitment,” in *2017 International Conference on Energy, Power and Environmental Engineering (ICEPEE 2017)*, Shanghai, 2017.
- [4] Erik Ela, Michael Milligan and Brendan Kirby, “Operating Reserves and Variable Generation: A comprehensive review of current strategies, studies, and fundamental research on the impact that increased penetration of variable renewable generation has on power system operating reserves.,” National Renewable Energy Laboratory, Colorado, USA, August 2011.
- [5] HomerEnergy, Hybrid Optimization of Multiple Electric Renewables Software Help Manual, <https://www.homerenergy.com>, 2012.
- [6] K. Oueilidis, K. N. Malamaki, K. Gallos, A. Tsitsimelis, C. Dikaiakos, S. Gkavanoudis, M. Cvetkovic, J. Mauricio, J.M.M. Ortega, J.LM. Ramos, G. Papaioannou and C. Demoulias, “Ancillary Services Market Design in Distribution Networks: Review and Identification of Barriers,” *Energies*, Vols. 13, no. 4, p. 917, 2020.
- [7] Paul Denholm, Daniel C. Steinberg, Aaron Bergman and David Rosner, “Maintaining Reliability in the Modern Power System,” U.S. Department of Energy's Office of Energy Policy and Systems Analysis (DOE-EPISA), Washington D.C., 2016.
- [8] S. Muller, M Deicke and Rik W. De Doncker, “Doubly Fed Induction Generator Systems for Wind Turbines,” *IEEE Industry Applications Magazine*, Vols. 8, no.4, pp. 26-33, 2002.
- [9] Al-Hinai and Amer S, Voltage collapse prediction for interconnected power systems, Statler College of Engineering and Mineral Resources: M.Sc. Graduate Theses, Dissertations and Problem Reports. 1065, 2000.
- [10] Xue Y., “Towards space-time cooperative defence framework against blackouts in China.,” in *In the Proceedings of the 2007 IEEE Power Engineering Society General Meeting*, Tampa, FL, USA, 2007.

- [11] Isaiah Adebayo, Adisa Jimoh and Adedayo Yusuff, “Techniques for the Identification of Critical Nodes Leading to Voltage Collapse in a Power System,” *International Journal of Emerging Electric Power Systems*, vol. 19, no. 2, 2018.
- [12] John W. Simpson-Porco and Francesco Bullo, “Distributed Monitoring of Voltage Collapse Sensitivity Indices,” *IEEE Transactions on Smart Grid*, vol. 7, no. 4, pp. 1979 - 1988, 2016.
- [13] Mir Sayed Shah Danish, Tomonobu Senjyu, Sayed Mir Shah Danish, N.R. Sabory, Narayanan K and Mandal Paras, “Recap of Voltage Stability Indices in the Past Three Decades,” *Energies*, vol. 12, no. 8, p. 1544, 2019.
- [14] Hameedullah Zaheb, Mir Sayed Shah Danish, Tomonobu Senjyu , Mikael Ahmadi, Abdul Malik Nazari, Mohebullah Wali, Mahdi Khosravy and Paras Mandal, “A Contemporary Novel Classification of Voltage Stability Indices,” *Applied Sciences*, vol. 10, p. 1639, 2020.
- [15] Tajudeen H. Sikiru, Adisa A. Jimoh and John T. Agee, “Inherent Structural Characteristic Indices of Power System Networks,” *International Journal of Electrical Power and Energy System*, vol. 47, pp. 218-224, 2013.
- [16] Kalyan Kumar Dr. and B., “Chapter 1: Power System Stability and Control,” Chennai, Indian Institute of Technology Madras, 2014, pp. 1-4.
- [17] Hassan Haes Alhelou, Mohamad Esmail Hamedani-Golshan, Takawira Cuthbert Njenda and Pierluigi Siano, “Survey on Power System Blackout and Cascading Events: Research Motivations and Challenges.,” *Energies*, vol. 12, no. 682, pp. 1-28, 2019.
- [18] S.G. Satimburwa, C. Ndlhovu, R.H. Marais and M. Kibido, “Technical Report: Generation Connection Capacity Assessment of the 2022 Transmission Network,” Eskom Transmission Division, Megawatt Park, Johannesburg., 2018.
- [19] Juan-Juan Wang, Wen-Lei Zhao, Wei-Dong Li and Yun-Li Zhao, “The Compare and Analysis of the Allocation Methods of the Contingency Reserves,” *Procedia Engineering*, vol. 29, pp. 1921-1925, 2012.
- [20] S.A Subramanyam, X. Zhang, J. Wu and H. Song, “Dynamic Analysis of Operating Reserve Demand Curve in Energy-Only Electricity Markets,” in *IEEE Innovative Smart Grid Technologies - Asia (ISGT Asia)*, August 2019.
- [21] Sikiru T.H., Jimoh A.A., Hamam Y., Agee J.T., and Ceschi R., “Voltage Profile improvement based on network structural characteristics,” in *6th IEEE Transmission and distribution Latin America Conference*, Montevideo, Uruguay, 2012.

- [22] Thukaram Dhadbanjan and Vyjayanthi Chintamani, "Evaluation of Suitable Locations for Generation Expansion in Restructured Power Systems: A Novel Concept of T-index," *International Journal of Emerging Electric Power Systems*, Vols. 10, , no. 1, 2009.
- [23] Sikiru T.H, Jimoh A.A, Hamam Y, Agee J.T and Ceschi R, "Classifications of networks based on inherent structural characteristics," in *6th IEEE/PES Transmission and Distribution Latin America Conference and Exposition (T&D-LA)*, Montevideo, Uruguay, 2012.
- [24] Yesuratnam G and Thukaram D, "Congestion management in open access based on relative electrical distances using voltage stability criteria.," *Electrical Power Systems Research*, vol. 77, no. 12, pp. 1608-1618, October 2007.
- [25] Vishaka K, Thukaram D and Lawrence Jenkins, "Transmission charges of power contracts based on relative electrical distances in open access," *Electrical Power Systems Research*, vol. 70, no. 2, pp. 153-161, 2004.
- [26] Aman M.M., Jasmon G.B., Mokhlis, H., Bakar and A.H.A., "Optimal placement and sizing of a DG based on a new power stability index and line losses.," *International Journal of Electrical Power & Energy Systems*, vol. 43, no. 1, pp. 1296-1304, 2012.
- [27] Yang C.F., Lai G.G., Lee C.H., Su C.T. and Chang G.W., "Optimal setting of reactive compensation devices with an improved voltage stability index for voltage stability enhancement," *International Journal of Electrical Power & Energy Systems*, vol. 37, no. 1, pp. 50-57, 2012.
- [28] Chakravorty M. and Das D., "Voltage stability analysis of radial distribution networks," *International Journal of Electrical Power & Energy Systems*, vol. 23, no. 2, pp. 129-135, 2001.
- [29] Balamourougan V., Sidhu T.S. and Sachdev M.S., "Technique for online prediction of voltage collapse," *IET Proceedings - Generation Transmission and Distribution*, vol. 151, no. 4, pp. 453-460, 2004.
- [30] Chen H., Jiang T., Yuan H., Jia H., Bai L. and Li F., "Wide-area measurement-based voltage stability sensitivity and its application in voltage control," *International Journal of Electrical Power & Energy Systems*, vol. 88, no. 12, pp. 87-98, 2017.
- [31] Li H., Zhou L., Mao M. and Zhang Q., "Three-layer voltage/Var control strategy for PV cluster considering steady-state voltage stability.," *Journal of Cleaner Production*, vol. 217, no. 1, 2019.
- [32] Tang L. and McCalley J., "Quantitative transient voltage dip assessment of contingencies using trajectory sensitivities.," *International Journal of Electrical Power & Energy Systems*, vol. 61, pp. 298-304, 2014.

- [33] P.Guimaraes, U Fernandez, T.Ocariz, F.W. Mohn and A.C.Z. de Souza, "QV and PV curves as a planning tool of analysis," in *4th International Conference on Electric Utility Deregulation and Restructuring and Power Technologies (DRPT)*, Weihai, Shandong, 2011.
- [34] Xiao Y and Wang Y., "Reactive power optimal control of a wind farm for minimizing collector system losses.," *Energies*, vol. 3177, no. 11, p. 11, 2018.
- [35] Hai T.P., Cho H., Chung I.Y., Kang H.K., Cho J. and Kim J., "A novel voltage control scheme for low-voltage DC distribution systems using multi-agent systems," *Energies*, vol. 41, p. 10, 2017.
- [36] Ghaffarianfar M. and Hajizadeh A., "Voltage Stability of Low-Voltage Distribution Grid with High Penetration of Photovoltaic Power Units.," *Energies*, vol. 11, no. 8, 2018.
- [37] Badrul H. Chowdhury and Carson W. Taylor, "Voltage Stability Analysis: V-Q Power Flow Simulation Versus Dynamic Simulation," in *IEEE Transactions on power systems*, Rolla-Missouri, November 2000.
- [38] Sikiru T.H., Andisa Jimoh, Agee J.T, "Optimal location of network devices using a novel inherent network topology based technique," in *IEEE AFRICON*, Livingstone, Zambia., 2011.
- [39] Sikiru T.H, Jimoh A.A., Hamam Y., Agee J.T. and Ceschi R., "Reactive power reserve improvement using power systems inherent structural characteristics," in *Asia-Pacific Power and Energy Engineering Conference (APPEEC 2013)*, Beijing, China., 2013.
- [40] B.Gao, G.K. Morison and P. Kundur, "Voltage stability evaluation using modal analysis," *IEEE Transactions on Power Systems*, vol. 7, no. 4, pp. 1529-1542, Nov. 1992.

APPENDIX A

MATLAB CODE

```
% IEEE 14 BUS SYSTEM.  
% Program to form Admittance Bus Formation with Transformer Tap setting
```

```
function [Y] = y_matrix14bus  
linedata = linedata14bus; % Calling "linedata14" for Linedata14bus.m..  
fb = linedata(:,2); % From bus number...  
tb = linedata(:,3); % To bus number...  
r = linedata(:,4); % Resistance, R...  
x = linedata(:,5)+linedata(:,8); % Reactance, X...  
b = linedata(:,6); % Ground Admittance, B/2...  
a = linedata(:,7); % Tap setting value..  
z = r + j*x; % Z matrix...  
y = 1./z; % To get inverse of each element...  
b = j*b; % Make B imaginary...  
nbus = max(max(fb),max(tb)); % no. of buses...  
nbranch = length(fb); % no. of branches...  
Y = zeros(nbus,nbus); % Initialise YBus...  
% Formation of the Off Diagonal Elements...  
for k=1:nbranch  
Y(fb(k),tb(k)) = Y(fb(k),tb(k))-y(k)/a(k);  
Y(tb(k),fb(k)) = Y(fb(k),tb(k));  
end  
% Formation of Diagonal Elements....  
for m =1:nbus  
for n =1:nbranch  
if fb(n) == m  
Y(m,m) = Y(m,m) + y(n)/(a(n)^2) + b(n);  
elseif tb(n) == m  
Y(m,m) = Y(m,m) + y(n) + b(n);  
end  
end  
end  
Y % Bus Admittance Matrix..  
return;
```

```
*****  
function [linedata14] = linedata14bus  
clear;clc  
B1_B2=0.00;  
B2_B3=0;  
B2_B6=0;  
B1_B8=0;  
B2_B8=0;  
B3_B6=0;  
B6_B8=0;  
B8_B4=0;  
B6_B7=0;  
B7_B5=0;  
B6_B9=0;  
B7_B9=0;  
B9_B10=0;  
B4_B11=0;  
B4_B12=0;  
B4_B13=0;  
B9_B14=0;  
B10_B11=0;  
B12_B13=0;  
B13_B14=0;
```

```

% Line Data for IEEE 14 bus system
%
linedata14 = [ 1 1 2 0.01938 0.05917 0.02640 1 B1_B2;
2 2 3 0.04699 0.19797 0.02190 1 B2_B3;
3 2 6 0.05811 0.17632 0.01870 1 B2_B6;
4 1 8 0.05403 0.22304 0.02460 1 B1_B8;
5 2 8 0.05695 0.17388 0.01700 1 B2_B8;
6 3 6 0.06701 0.17103 0.01730 1 B3_B6;
7 6 8 0.01335 0.04211 0.00640 1 B6_B8;
8 8 4 0.00000 0.25202 0.00000 0.932 B8_B4;
9 6 7 0.00000 0.20912 0.00000 0.978 B6_B7;
10 7 5 0.00000 0.17615 0.00000 1 B7_B5;
11 6 9 0.00000 0.55618 0.00000 0.969 B6_B9;
12 7 9 0.00000 0.11001 0.00000 1 B7_B9;
13 9 10 0.03181 0.08450 0.00000 1 B9_B10;
14 4 11 0.09498 0.19890 0.00000 1 B4_B11;
15 4 12 0.12291 0.25581 0.00000 1 B4_B12;
16 4 13 0.06615 0.13027 0.00000 1 B4_B13;
17 9 14 0.12711 0.27038 0.00000 1 B9_B14;
18 10 11 0.08205 0.19207 0.00000 1 B10_B11;
19 12 13 0.22092 0.19988 0.00000 1 B12_B13;
20 13 14 0.17093 0.34802 0.00000 1 B13_B14];

return;
V = y_matrix14bus;
clc; % clears/Prevents Y matrix , that we called from script y_matrix14bus from showing again.
e = V(1:5,1:5);
f = V(1:5,6:14);
g = V(6:14,1:5);
h = V(6:14,6:14);
G_region = e-f*inv(h)*g;
eig(G_region);
display('Generator Attraction Region')
abs(eig(G_region))
L_region = h-g*inv(e)*f;
eig(L_region);
display('Load attraction Region')
abs(eig(L_region))
display('Generator affinity')
abs(-inv(e)*f)
display('Ideal Generator Contribution')
abs(-inv(h)*g)

```

```

% SOUTHERN INDIAN 10 BUS SYSTEM.
function [linedata10] = linedata10bus
clear;clc
B1_B2=0;
B3_B8=0;
B3_B9=0;
B7_B5=0;
B2_B10=0;
B10_B6=0;
B6_B7=0;
B1_B4=0;
B7_B4=0;
B7_B9=0;
B1_B5=0;
B5_B8=0;
% Line Data for Southern Indian 10bus system
%      Line No From to      R          X      B/2  T  FACTs
linedata10 = [1   1   2  0.00477   0.05103   0    1  B1_B2;
              2   3   8  0.00297   0.03706   0    1  B3_B8;
              3   3   9  0.00145   0.01802   0    1  B3_B9;
              4   7   5  0.0043    0.04770   0    1  B7_B5;
              5   2  10  0.00676   0.09429   0    1  B2_B10;
              6  10   6  0.00546   0.06794   0    1  B10_B6;
              7   6   7  0.00040   0.0040    0    1  B6_B7;
              8   1   4  0.00569   0.06008   0    1  B1_B4;
              9   7   4  0.00589   0.05995   0    1  B7_B4;
             10   7   9  0.00289   0.03603   0    1  B7_B9;
             11   1   5  0.00272   0.02872   0    1  B1_B5;
             12   5   8  0.00388   0.04834   0    1  B5_B8];

return;
function [Y] = y_matrix10bus
linedata = linedata10bus; % Calling "linedata14" for Linedata14bus.m...
fb = linedata(:,2); % From bus number...
tb = linedata(:,3); % To bus number...
r = linedata(:,4); % Resistance, R...
x = linedata(:,5)+linedata(:,8); % Reactance, X...
b = linedata(:,6); % Ground Admittance, B/2...
a = linedata(:,7); % Tap setting value..
z = r + j*x; % Z matrix...
y = 1./z; % To get inverse of each element...
b = j*b; % Make B imaginary...

nbus = max(max(fb),max(tb)); % no. of buses...
nbranch = length(fb); % no. of branches...
Y = zeros(nbus,nbus); % Initialise YBus...
% Formation of the Off Diagonal Elements...
for k=1:nbranch
Y(fb(k),tb(k)) = Y(fb(k),tb(k))-y(k)/a(k);

```

```

Y(tb(k),fb(k)) = Y(fb(k),tb(k));
end
% Formation of Diagonal Elements....
for m =1:nbus
for n =1:nbranch
if fb(n) == m
Y(m,m) = Y(m,m) + y(n)/(a(n)^2) + b(n);
elseif tb(n) == m
Y(m,m) = Y(m,m) + y(n) + b(n);
end
end
end
Y % Bus Admittance Matrix..
return;

*****
U = y_matrix10bus;
clc; % clears/Prevents Y matrix , that we called from script y_matrix14bus from showing again.
e = U(1:3,1:3);
f = U(1:3,4:10);
g = U(4:10,1:3);
h = U(4:10,4:10);
G_region = e-f*inv(h)*g;
eig(G_region);
display('Generator Attraction Region')
abs(eig(G_region))
L_region = h-g*inv(e)*f;
eig(L_region);
display('Load attraction Region')
abs(eig(L_region))
display('Generator affinity')
abs(-inv(e)*f)
display ('Ideal Generator Contribution')
abs(-inv(h)*g)

-----

% Reduced Jacobian matrix eigen value analysis.

clear;clc
Data10;
Y; % Calling ybusppg.m to get Y-Bus Matrix..
busd = busdata_1; % Calling busdatas..
BMva = 100; % Base MVA..
bus = busdata_1(:,1); % Bus Number..
type = busd(:,10); % Type of Bus 1-Slack, 2-PV, 3-PQ..
V = busd(:,2); % Specified Voltage..
del = busd(:,3); % Voltage Angle..
Pg = busd(:,4)/BMva; % PGi..
Qg = busd(:,5)/BMva; % QGi..
Pl = busd(:,6)/BMva; % PLi..
Ql = busd(:,7)/BMva; % QLi..
Qmin = busd(:,8)/BMva; % Minimum Reactive Power Limit..
Qmax = busd(:,9)/BMva; % Maximum Reactive Power Limit..
P = Pg - Pl; % Pi = PGi - PLi..
Q = Qg - Ql; % Qi = QGi - QLi..
Psp = P; % P Specified..
Qsp = Q; % Q Specified..
G = real(Y); % Conductance matrix..
B = imag(Y); % Susceptance matrix..

```

```

pv = find(type == 2 | type == 1); % PV Buses..
pq = find(type == 3); % PQ Buses..
npv = length(pv); % No. of PV buses..
npq = length(pq); % No. of PQ buses..
Tol = 1;
Iter = 1;
while (Tol > 0.00001) % Iteration starting..

    P = zeros(nbus,1);
    Q = zeros(nbus,1);
    % Calculate P and Q
    for i = 1:nbus
        for k = 1:nbus
            P(i) = P(i) + V(i)* V(k)*(G(i,k)*cos(del(i)-del(k)) + B(i,k)*sin(del(i)-del(k)));
            Q(i) = Q(i) + V(i)* V(k)*(G(i,k)*sin(del(i)-del(k)) - B(i,k)*cos(del(i)-del(k)));
        end
    end
    % Checking Q-limit violations..
    if Iter <= 7 && Iter > 2 % Only checked up to 7th iterations..
        for n = 2:nbus
            if type(n) == 2
                QG = Q(n)+Ql(n);

                if QG < Qmin(n)
                    V(n) = V(n) + 0.01;
                elseif QG > Qmax(n)
                    V(n) = V(n) - 0.01;
                end
            end
        end
    end
    % Calculate change from specified value
    dPa = Psp-P;
    dQa = Qsp-Q;
    k = 1;
    dQ = zeros(npq,1);
    for i = 1:nbus
        if type(i) == 3
            dQ(k,1) = dQa(i);
            k = k+1;
        end
    end
    dP = dPa(2:nbus);

    M = [dP; dQ]; % Mismatch Vector
    % Jacobian
    % J1 - Derivative of Real Power Injections with Angles..
    J1 = zeros(nbus-1,nbus-1);
    for i = 1:(nbus-1)
        m = i+1;
        for k = 1:(nbus-1)
            n = k+1;
            if n == m
                for n = 1:nbus
                    J1(i,k) = J1(i,k) + V(m)* V(n)*(-G(m,n)*sin(del(m)-del(n)) + B(m,n)*cos(del(m)-del(n)));
                end
            end
        end
    end
end

```

```

        end
        J1(i,k) = J1(i,k) - V(m)^2*B(m,m);
    else
        J1(i,k) = V(m)* V(n)*(G(m,n)*sin(del(m)-del(n)) - B(m,n)*cos(del(m)-del(n)));
    end
end
end
end
% J2 - Derivative of Real Power Injections with V..
J2 = zeros(nbus-1,npq);
for i = 1:(nbus-1)
    m = i+1;
    for k = 1:npq
        n = pq(k);
        if n == m
            for n = 1:nbus
                J2(i,k) = J2(i,k) + V(n)*(G(m,n)*cos(del(m)-del(n)) + B(m,n)*sin(del(m)-del(n)));
            end
            J2(i,k) = J2(i,k) + V(m)*G(m,m);
        else
            J2(i,k) = V(m)*(G(m,n)*cos(del(m)-del(n)) + B(m,n)*sin(del(m)-del(n)));
        end
    end
end
end
% J3 - Derivative of Reactive Power Injections with Angles..
J3 = zeros(npq,nbus-1);
for i = 1:npq
    m = pq(i);
    for k = 1:(nbus-1)
        n = k+1;
        if n == m
            for n = 1:nbus
                J3(i,k) = J3(i,k) + V(m)* V(n)*(G(m,n)*cos(del(m)-del(n)) + B(m,n)*sin(del(m)-del(n)));
            end
            J3(i,k) = J3(i,k) - V(m)^2*G(m,m);
        else
            J3(i,k) = V(m)* V(n)*(-G(m,n)*cos(del(m)-del(n)) - B(m,n)*sin(del(m)-del(n)));
        end
    end
end
end
% J3 - Derivative of Reactive Power Injections with Angles..
J3 = zeros(npq,nbus-1);
for i = 1:npq
    m = pq(i);
    for k = 1:(nbus-1)
        n = k+1;
        if n == m
            for n = 1:nbus
                J3(i,k) = J3(i,k) + V(m)* V(n)*(G(m,n)*cos(del(m)-del(n)) + B(m,n)*sin(del(m)-del(n)));
            end
            J3(i,k) = J3(i,k) - V(m)^2*G(m,m);
        else
            J3(i,k) = V(m)* V(n)*(-G(m,n)*cos(del(m)-del(n)) - B(m,n)*sin(del(m)-del(n)));
        end
    end
end
end
% J4 - Derivative of Reactive Power Injections with V..
J4 = zeros(npq,npq);
for i = 1:npq
    m = pq(i);
    for k = 1:npq
        n = pq(k);
        if n == m
            for n = 1:nbus
                J4(i,k) = J4(i,k) + V(n)*(G(m,n)*sin(del(m)-del(n)) - B(m,n)*cos(del(m)-del(n)));
            end
        end
    end
end
end

```

```

        end
        J4(i,k) = J4(i,k) - V(m)*B(m,m);
    else
        J4(i,k) = V(m)*(G(m,n)*sin(del(m)-del(n)) - B(m,n)*cos(del(m)-del(n)));
    end
end
end
end
J=[J1 J2;J3 J4];
% Jacobian Matrix..
X = inv(J)*M; % Correction Vector
dTh = X(1:nbus-1); % Change in Voltage Angle..
dV = X(nbus:end); % Change in Voltage Magnitude..
% Updating State Vectors..
del(2:nbus) = dTh + del(2:nbus); % Voltage Angle..
k = 1;
for i = 2:nbus
    if type(i) == 3
        V(i) = dV(k) + V(i); % Voltage Magnitude..
        k = k+1;
    end
end
end

Iter = Iter + 1;
Tol = max(abs(M)); % Tolerance..

JR1=J4-J3*inv(J1)*J2;
abs(eig(JR1))
end
P;
Q;
G;
B;
V;
del;
%Loss Calculation
Vs=V(fb);
Vr=V(tb);
dels=del(fb);
delr=del(tb);
G=real(y);
for i=1:10

P1(i)=G(i)*((Vs(i)^2)+(Vr(i)^2)-2*Vs(i)*Vr(i)*cos(dels(i)-delr(i)));

end
sum(P1)

```

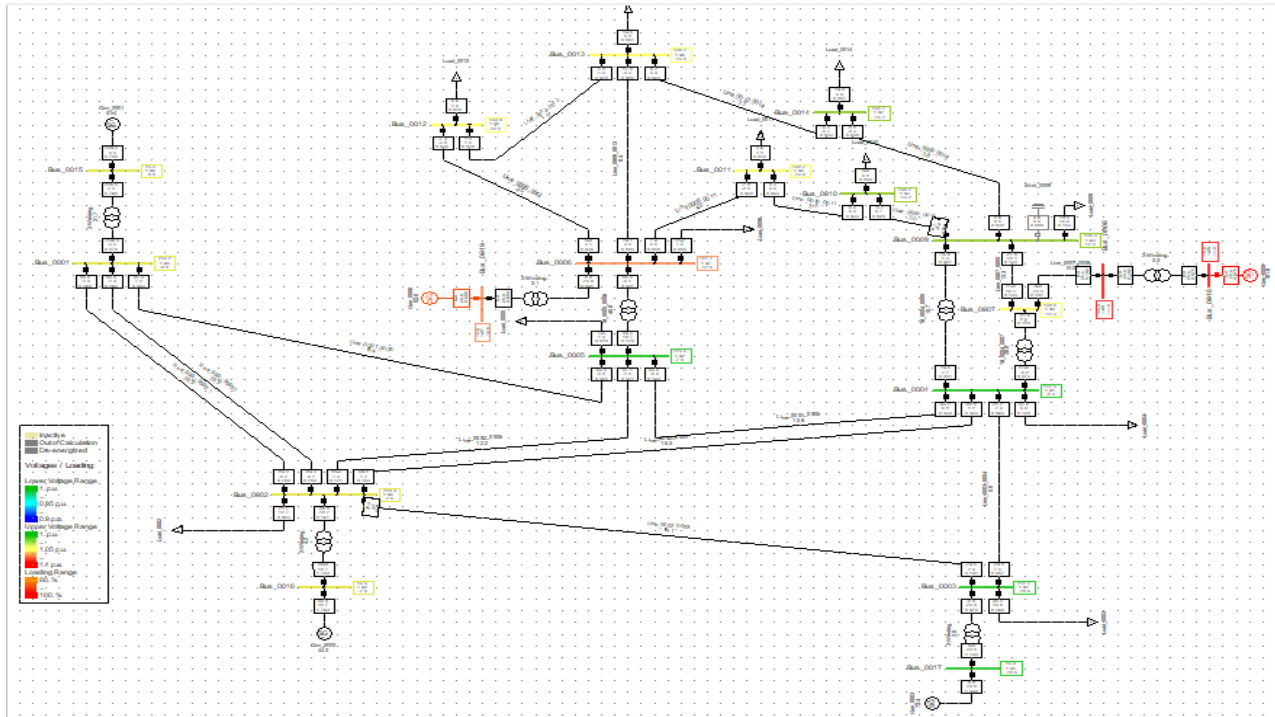
APPENDIX B

LINE DATA FOR 10 BUS SOUTHERN INDIAN EQUIVALENT NETWORK SYSTEM			
Sending end Bus	Receiving end Bus	R (per unit)	X (per unit)
1	2	0.00477	0.05103
3	8	0.00297	0.03706
3	9	0.00297	0.01802
7	5	0.00145	0.04770
2	10	0.00430	0.09429
10	6	0.00676	0.06794
6	7	0.00546	0.00400
1	4	0.0004	0.06008
7	4	0.00589	0.05995
7	9	0.00289	0.03603
1	5	0.00272	0.02872
5	8	0.00388	0.04834

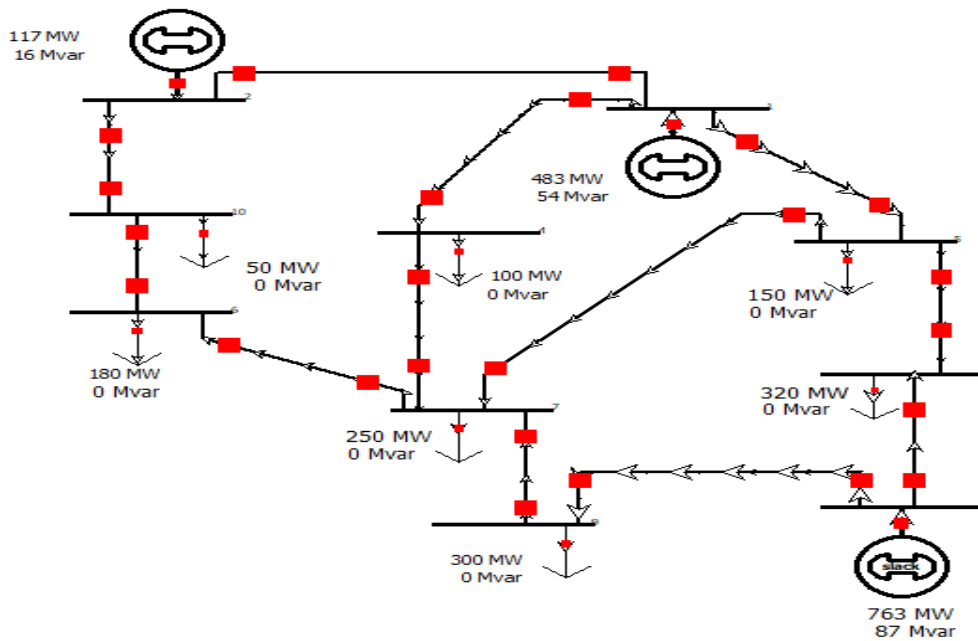
IEEE 14 BUS SYSTEM PQ BASE CASE LOAD DATA		
Bus No.	Real power (per unit)	Reactive power (per unit)
1	0.00	0.00
2	0.217	0.127
3	0.942	0.19
4	0.478	0.04
5	0.076	0.016
6	0.112	0.075
7	0.00	0.00
8	0.00	0.00
9	0.295	0.166
10	0.09	0.058
11	0.035	0.018
12	0.061	0.016
13	0.135	0.058
14	0.149	0.05

LINE DATA FOR IEEE 14 BUS SYSTEM					
Sending end Bus	Receiving end Bus	Resistance (per unit)	Reactance (per unit)	Half Susceptance (per unit)	Transformer tap
1	2	0.01938	0.05917	0.0264	1
2	3	0.04699	0.19797	0.0219	1
2	4	0.05811	0.17632	0.0187	1
1	5	0.05403	0.22304	0.0246	1
2	5	0.05695	0.17388	0.0170	1
3	4	0.06701	0.17103	0.0173	1
4	5	0.01335	0.04211	0.0064	1
5	6	0	0.25202	0	0.932
4	7	0	0.20912	0	0.978
7	8	0	0.17615	0	1
4	9	0	0.55618	0	0.969
7	9	0	0.11001	0	1
9	10	0.03181	0.0845	0	1
6	11	0.09498	0.1989	0	1
6	12	0.12291	0.25581	0	1
6	13	0.06615	0.13027	0	1
9	14	0.12711	0.27038	0	1
10	11	0.08205	0.19207	0	1
12	13	0.22092	0.19988	0	1
13	14	0.17093	0.34802	0	1

IEEE 14 BUS SYSTEM NETWORK IN DigSILENT POWERFACTORY WITH BASE CASE
LOADING

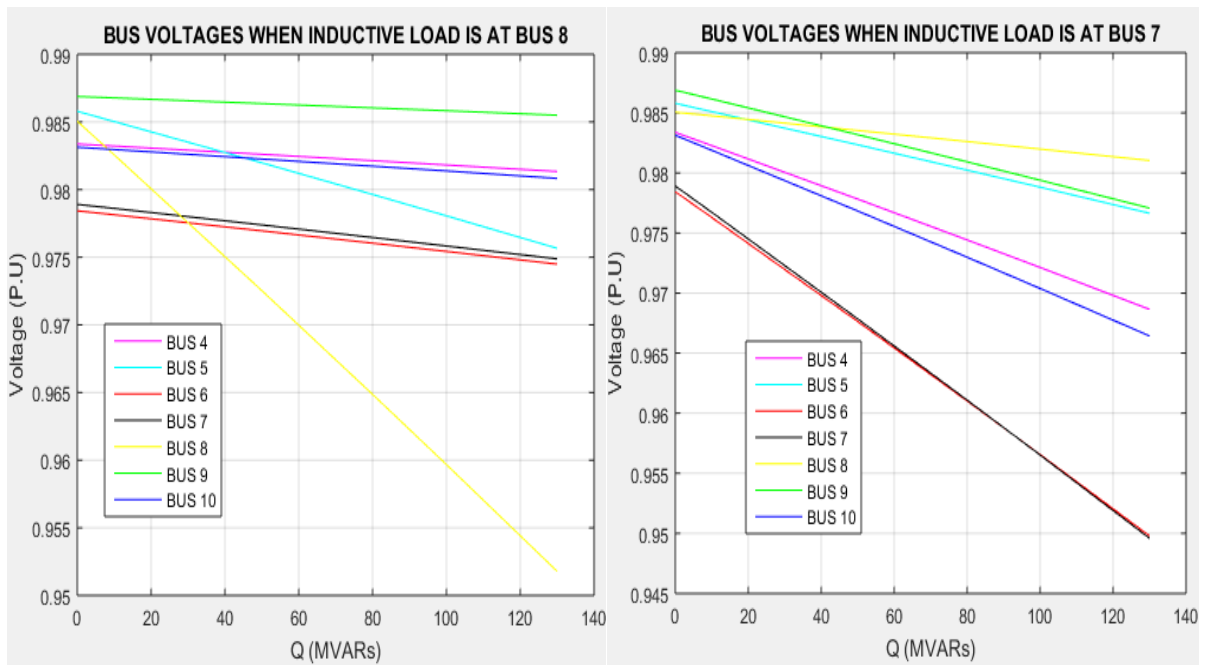
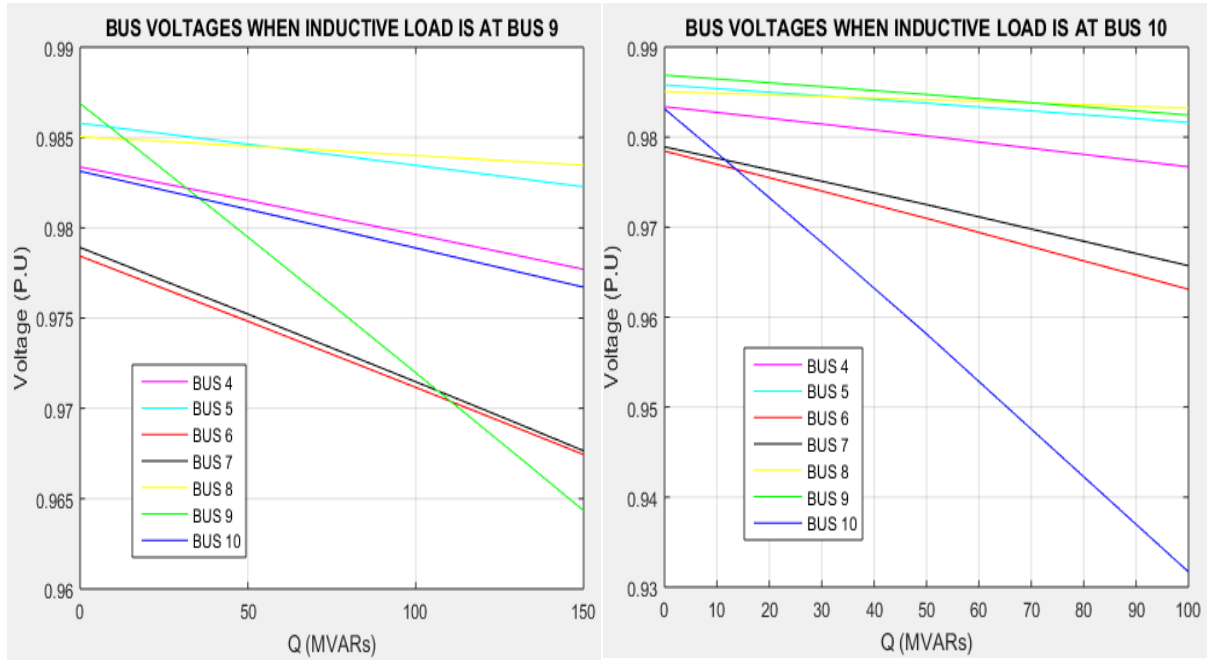


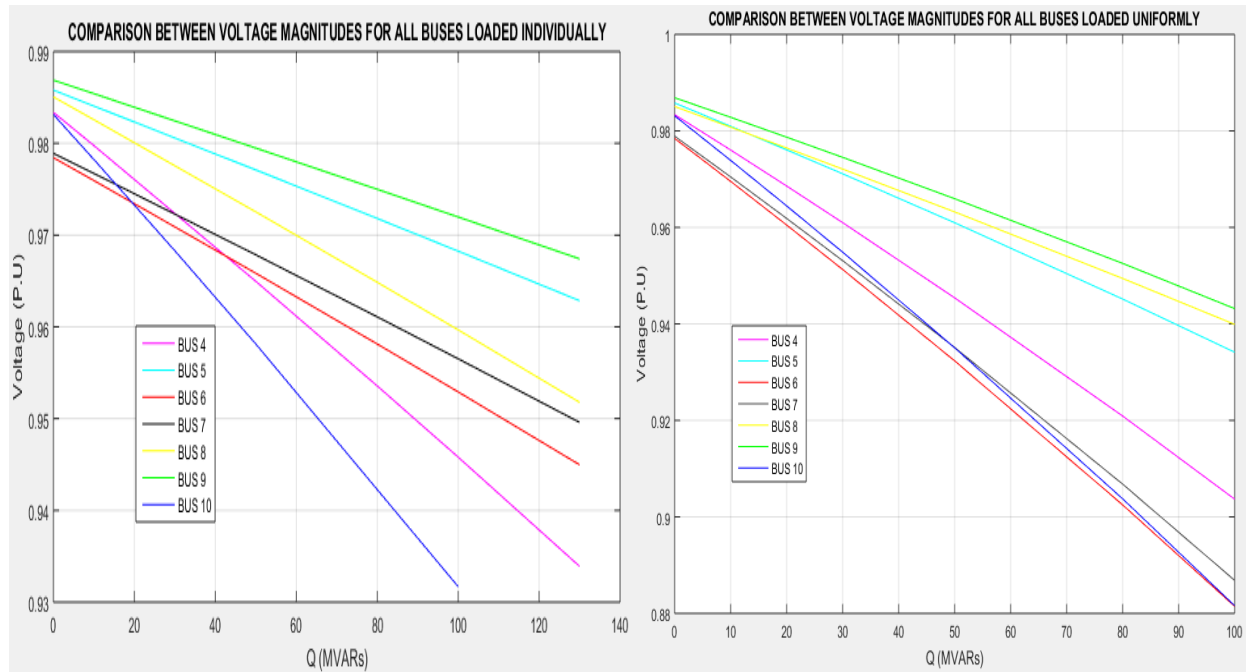
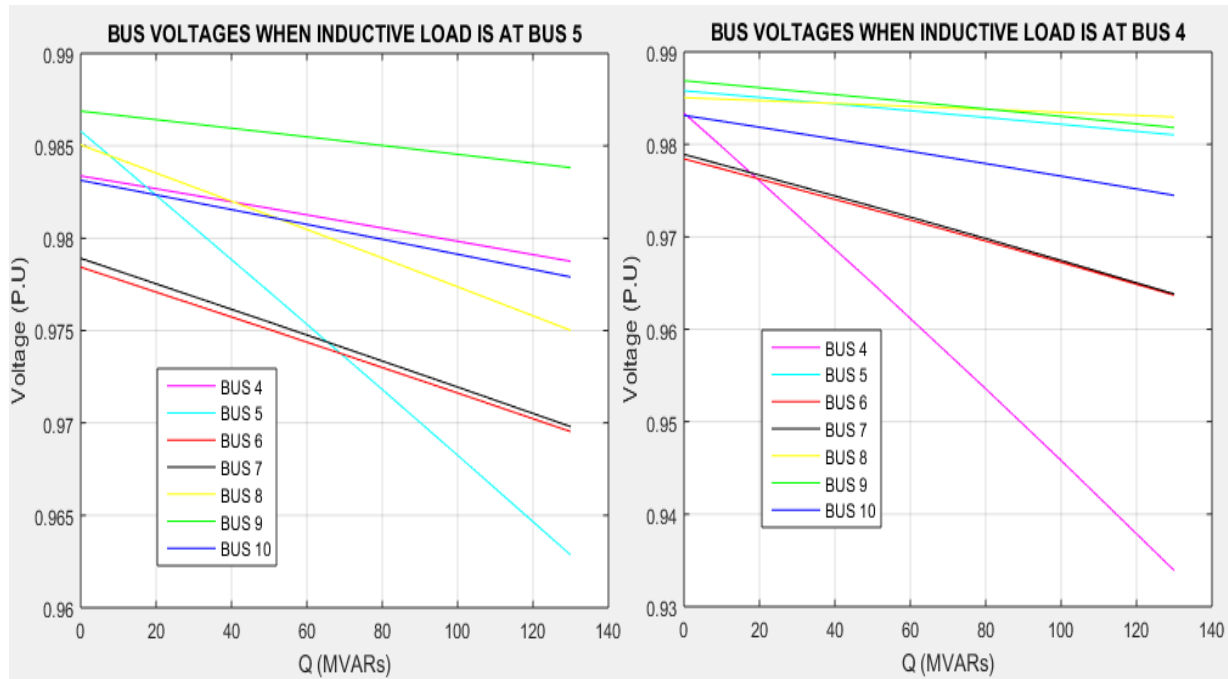
SOUTHERN INDIAN 10 BUS SYSTEM IN POWERWORLD SIMULATOR WITH MW BASE
CASE LOADING.



APPENDIX C

GRAPHS OF SINGLE BUS LOADING IN SOUTHERN INDIAN NETWORK SYSTEM





APPENDIX D

An exhaustive illustration and type of voltage stability indices [13]

	Type	Index	Abbreviation	Calculation
System parameters (variables)-based		L Index	L	$L = \text{MAX}_{j \in \alpha_L} \left 1 - \frac{\sum_{i \in \alpha_G} F_{ij} V_i}{V_j} \right $
		Power Stability Index	PSI	$PSI = \frac{4r_{ij}(P_L - P_G)}{\ V_i\ \cos(\theta - \delta)}^2$
		Voltage Deviation Index	VDI	$VDI_j = 1 - V_j $
		Stability Index	SI	$SI(m2) = \{ V(m1) ^4 - 4.0\{P(m2)x(jj) - Q(m2)r(jj)\}^2 - 4.0\{P(m2)r(jj) + Q(m2)x(jj)\} V(m1) ^2 \}$
	For Bus	Voltage Collapse Prediction Index	$VCPI_{kth\ bus}$	$VCPI_{kth\ bus} = 1 - \frac{\sum_{m=1}^N V_m }{m \neq k} V_k$
		Sensitivity Analysis	SA	$\frac{\Delta V_i / \Delta Q_i}{\Delta V_i / \Delta P_i}$
		Bus Participation Factor	BPF	
		Voltage Stability Index	VSI	$VSI_i = \left[1 + \left(\frac{I_i}{V_i} \right) \left(\frac{\Delta V_i}{\Delta I_i} \right) \right]^\alpha$
		Equivalent Node Voltage Collapse Index	$ENVCI$	$ENVCI = 2(e_k e_n + f_k f_n) - (e_k^2 + e_n^2)$
		Voltage Collapse Index	VCI	$VCI_i = \left[1 + \left(\frac{I_i \Delta V_i}{V_i \Delta I_i} \right) \right]^\alpha$
	Improved Voltage Stability Index	$IVSI$	$\frac{-4 \sum_{j=0}^n (G_{ij} - B_{ij})(P_i + Q_i)(IVSI \leq 1)}{\left[\sum_{j=1}^n V_j [G_{ij}(\cos \delta_{ij} + \sin \delta_{ij}) - B_{ij}(\cos \delta_{ij} + \sin \delta_{ij})] \right]^2}$	
	Voltage Stability Factor	VSF	$VSF_{total} = \sum_{m=1}^{k-1} (2V_{m+1} - V_m)$	
	Voltage Instability Proximity Index	$VIPI$	$VIPI = \theta = \cos^{-1} \frac{Y(a)}{\ Y_s\ \ Y(a)\ }$	
For Line		L_{mn} Index	L_{mn}	$L_{mn} = \frac{4Qx}{\ V_s\ \sin(\theta - \delta)}^2$
		Line Voltage Factor	LQP	$LQP = 4 \left(\frac{X}{V_i} \right) \left(\frac{X}{V_i} P_i^2 + Q_i \right)$
		Line Index	L	$L = 4 \left[(x_{eg} P_{leg} - r_{eg} Q_{leg})^2 + x_{eg} Q_L + r_{eg} P_{leg} \right]$
				$VCPI(1) = \frac{P_i}{P_i(\max)}$
		Voltage Collapse Proximity Indicator	$VCPI$	$VCPI(2) = \frac{Q_i}{Q_i(\max)}$ $VCPI(3) = \frac{P_i}{P_i(\max)}$ $VCPI(4) = \frac{Q_i}{Q_i(\max)}$
		Novel Line Stability Index	$NLSI$	$NLSI_{ij} = \frac{R_{ij} P_j + X_{ij} Q_j}{0.25 V_i^2}$
		Fast Voltage Stability Index	$FVSI$	$FVSI_{ij} = \frac{4Z^2 Q_j}{V_i^2 x}$
		Critical Voltage	V_σ	$V_\sigma = \frac{E}{2 \cos \theta}$
		Power Transfer Stability Index	$PTSI$	$PTSI = \frac{2S_i Z_{Thev}(1 + \cos(\beta - \alpha))}{E_{Thev}^2}$
		Line Voltage Stability Index	$LVSI$	$LVSI = \frac{4rP_r}{V_s \cos(\theta - \delta)}^2$
	Critical Boundary Index	CBI	$CBI_{ik} = \sqrt{\Delta P_{ik}^2 + \Delta Q_{ik}^2}$	
	Line Voltage Stability Index	$LVSI$	$LVSI = \max(LVSI_j) \quad \forall j = 1, 2, 3, \dots, l$	
	Integrated Transmission Line Transfer Index	$ITLTI$	$P_R = -\frac{AV_R^2}{B} \cos(\beta - \alpha) + \frac{V_S V_R}{B} \cos(\beta - \alpha)$	

Jacobian matrix-based	Impedance Ratio Indicator		$\frac{Z_{ii}}{Z_i}$
	Minimum Eigenvalue and Right eigenvector method	RE	$\Delta V = \sum_i \frac{\xi_i \eta_i}{\lambda_i} \Delta Q$
	Minimum Singular value Predicting Voltage Collapse Test Function		$\begin{bmatrix} \Delta \theta \\ \Delta V \end{bmatrix} = \mathbf{V} \Sigma^{-1} \mathbf{U}^T \begin{bmatrix} \Delta F \\ \Delta G \end{bmatrix}$
			$\frac{V}{V_0}$
			$t_{cc} = e_c^T J J_{cc}^{-1} e_c $
	Tangent Vector Index	TVI	$TVI_i = \left \frac{dV_i}{d\lambda} \right ^{-1}$
Second-Order Index	i	$i = \frac{1}{i_0} \frac{\sigma_{max}}{d\sigma_{max}/d\lambda_{total}}$	
Integral Steady-State Margin	ISSM	$ISSM = \left \frac{I_c}{J_0} \right $	

Type	Index	Abbreviation	Calculation	
Phasor Measurement Units (PMU)-based	Local Measurement-based	Recursive Least Square	RLS	$x_k = x_{k-1} + G_k (y_k - H_k^T x_{k-1})$ $G_k = P_{k-1} H_k (\lambda I + H_k^T P_{k-1} H_k)^{-1}$ $P_k = \frac{1}{\lambda} (I - G_k H_k^T) P_{k-1}$
		Voltage Instability Predictor	VIP	$\Delta S = \frac{(V_k - Z_{Th} I_k)^2}{4Z_{Th}}$
		Voltage Stability Load Bus Index	VSLBI	$VSLBI_k = \frac{ V_i(k) }{ \Delta V_i(k) }$
		Approximate Approach		$V_{Li} = E_{eq,i} - Z_{eq} I_{Li}$ $Z_{eq} = Z_{LLii}$
	Simplified Voltage Stability Index	SVSI	$SVSI_i = \frac{\Delta V_i}{\beta V_i}$	
	Observability-based	Voltage Collapse Proximity Indicator	VCPI	$VCPI_{kth \ bus} = \left 1 - \frac{\sum_{m=1}^N V_m}{V_k} \right $
		Margin Voltage Stability Index	MVSI	$VSI = \min \left(\frac{P_{margin}}{P_{max}}, \frac{Q_{margin}}{Q_{max}}, \frac{S_{margin}}{S_{max}} \right)$
	Sensitivity Related Eigenvalue		$S_{Qgq} = -g_q^T (g_x^T)^{-1} \Delta_x Q_g$	